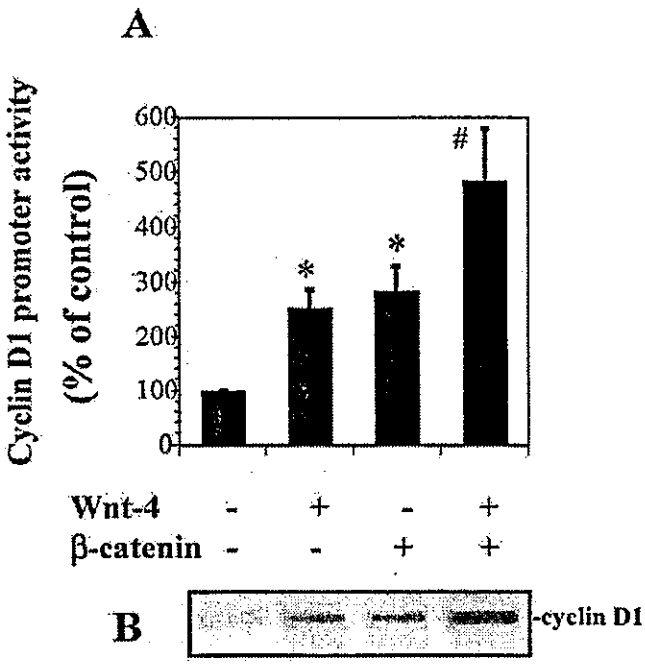

Figure 8. Effects of Wnt-4 and β-catenin on the transcriptional activity and protein expression of cyclin D1. (A) After co-transfecting the cells with cyclin D1 promoter-luciferase construct together with β-galactosidase reporter construct and expression vectors containing Wnt-4, β-catenin dN, or pCDNA3 (vector), they were incubated with DMEM medium without FCS. Cyclin D1 promoter luciferase activities were measured as described in the Materials and Methods section. Results are means ± SEM of four or five independent experiments. * $P < 0.05$; # $P < 0.01$. (B) LLC-PK1 cells were infected with Wnt-4, β-catenin dN plasmids, or pCDNA3 (vector) and incubated for 48 h. Whole cell lysates were separated by SDS-PAGE gels. Western blot analysis was used to detect the cyclin D1 protein levels.

Further studies will be necessary to gain a more precise understanding of the molecular mechanisms of renal recovery after ischemia/reperfusion injury.

Acknowledgments

We thank Drs. M. Eilers and K. Matsumoto for providing plasmids. An abstract of this work was presented at the 2001 Annual Meeting of the American Society of Nephrology, October 2001, San Francisco, CA.

References

1. Molitoris BA: Ischemic acute renal failure: exciting times at our fingertips. *Curr Opin Nephrol Hypertens* 7: 405–406, 1998
2. Bonventre JV: Mechanisms of ischemic acute renal failure. *Kidney Int* 43: 1160–1178, 1993
3. Safirstein R, DiMari J, Megyesi J, Price P: Mechanisms of renal repair and survival following acute injury. *Semin Nephrol* 18: 519–522, 1998
4. Bacallao R, Fine LG: Molecular events in the organization of renal tubular epithelium: From nephrogenesis to regeneration. *Am J Physiol* 257: F919–F924, 1989
5. Wallin A, Zhang G, Jones TW, Jaken S, Stevens JL: Mechanism of the nephrogenic repair response. Studies on proliferation and vimentin expression after 35S-1,2-dichlorovinyl-L-cysteine nephrotoxicity in vivo and in cultured proximal tubule epithelial cells. *Lab Invest* 66: 474–484, 1992
6. Witzgall R, Brown D, Schwarz C, Bonventre JV: Localization of proliferating cell nuclear antigen, vimentin, c-fos, and clusterin in the postischemic kidney. *J Clin Invest* 93: 2175–2188, 1994
7. Safirstein R: Gene expression in nephrotoxic and ischemic acute renal failure. *J Am Soc Nephrol* 4: 1387–1395, 1994
8. Megyesi J, Udvarhelyi N, Safirstein RL, Price PM: The p53-independent activation of transcription of p21 WAF1/CIP1/SDI1 after acute renal failure. *Am J Physiol* 270: F1211–F1216, 1996
9. Megyesi J, Safirstein RL, Price PM: Induction of p21WAF1/CIP1/SDI1 in kidney tubule cells affects the course of cisplatin-induced acute renal failure. *J Clin Invest* 101: 777–782, 1998
10. Kato J, Matsushime H, Hiebert SW, Ewen ME, Sherr CJ: Direct binding of cyclin D to the retinoblastoma gene product (pRb) and pRb phosphorylation by the cyclin D-dependent kinase CDK4. *Genes Dev* 7: 331–342, 1993
11. Sherr CJ, Kato J, Quelle DE, Matsuoka M, Roussel MF: D-type cyclins and their cyclin-dependent kinases: G1 phase integrators of the mitogenic response. *Cold Spring Harb Symp Quant Biol* 59: 11–19, 1994
12. Terada Y, Nakashima O, Inoshita S, Kuwahara M, Sasaki S, Marumo F: TGF-beta-activating kinase-1 inhibits cell cycle and expression of cyclin D1 and A in LLC-PK1 cells. *Kidney Int* 56: 1378–1390, 1999
13. Willert K, Nusse R: Beta-catenin: A key mediator of Wnt signaling. *Curr Opin Genet Dev* 8: 95–102, 1998
14. Miller JR, Hocking AM, Brown JD, Moon RT: Mechanism and function of signal transduction by the Wnt/beta-catenin and Wnt/Ca2+ pathway. *Oncogene* 18: 7860–7872, 1999
15. Stark K, Vainio S, Vassileva G, McMahon AP: Epithelial transformation of metanephric mesenchyme in the developing kidney regulated by Wnt-4. *Nature* 372: 679–683, 1994
16. Cadigan KM, Nusse R: Wnt signaling: A common theme in animal development. *Genes Dev* 11: 3286–3305, 1997
17. Behrens J, von KJ, Kuhl M, Bruhn L, Wedlich D, Grosschedl R, Birchmeier W: Functional interaction of beta-catenin with the transcription factor LEF-1. *Nature* 382: 638–642, 1996
18. Molenaar M, van de Wetering M, Oosterwegel M, Peterson MJ, Godsave S, Korinek V, Roose J, Destree O, Clevers H: XTcf-3 transcription factor mediates beta-catenin-induced axis formation in Xenopus embryos. *Cell* 86: 391–399, 1996
19. Tetsu O, McCormick F: Beta-catenin regulates expression of cyclin D1 in colon carcinoma cells. *Nature* 398: 422–426, 1999
20. Weide T, Bayer M, Koster M, Siebrasse JP, Peters R, Barnekow A: The Golgi matrix protein GM130: A specific interacting partner of the small GTPase rab1b. *EMBO Rep* 2:336–341, 2001
21. Denker BM, Smith BL Kuhajda FP, Agre P: Identification, purification, and partial characterization of a novel Mr 28,000 integral membrane protein form erythrocytes and renal tubules. *J Biol Chem* 263: 15634–15642, 1988
22. Yamamoto T, Sasaki S: Aquaporins in the kidney: Emerging new aspects. *Kidney Int* 54: 1041–1051, 1998
23. Nielsen S, Agre P: The aquaporin family of water channels in kidney. *Kidney Int* 48: 1057–1068, 1995
24. Terada Y, Tomita K, Homma MK, Nonoguchi H, Yang T, Yamada T, Yuasa Y, Krebs EG, Sasaki S, Marumo F: Sequential activation of Raf-1 kinase, mitogen-activated protein (MAP) kinase kinase, MAP kinase, and S6 kinase by hyperosmolality in renal cells. *J Biol Chem* 269: 31296–31301, 1994

25. Terada Y, Tomita K, Nonoguchi H, Yang T, Marumo F: Different localization and regulation of two types of vasopressin receptor messenger RNA in microdissected rat nephron segments using reverse transcription polymerase chain reaction. *J Clin Invest* 92: 2339–2345, 1993
26. Gibson UE, Heid CA, Williams PM: A novel method for real time quantitative RT-PCR. *Genome Res* 6: 995–1001, 1996
27. Heid CA, Stevens J, Livak KJ, Williams PM: Real time quantitative PCR. *Genome Res* 6: 986–994, 1996
28. Fort P, Marty L, Piechaczyk M, el SS, Dani C, Jeanteur P, Blanchard JM: Various rat adult tissues express only one major mRNA species from the glyceraldehyde-3-phosphate-dehydrogenase multigenic family. *Nucleic Acids Res* 13: 1431–1442, 1985
29. Solomon DL, Philipp A, Land H, Eilers M: Expression of cyclin D1 mRNA is not upregulated by Myc in rat fibroblasts. *Oncogene* 11: 1893–1897, 1995
30. Ishitani T, Ninomiya-Tsuji J, Nagai S, Nishita M, Meneghini M, Barker N, Waterman M, Bowerman B, Cleavers H, Shibuya H, Matsumoto K: The TAK1-NLK-MAPK related pathway antagonizes signaling between β-catenin and transcription factor TCF. *Nature* 399: 798–802, 1999
31. Terada Y, Yamada T, Nakashima O, Tamamori M, Ito H, Sasaki S, Marumo F: Overexpression of cell cycle inhibitors (p16INK4 and p21Cip1) and cyclin D1 using adenovirus vectors regulates proliferation of rat mesangial cells. *J Am Soc Nephrol* 8: 51–60, 1997
32. Nguyen HT, Thomson AA, Kogan BA, Baskin LS, Cunha GR: Expression of the Wnt gene family during late nephrogenesis and complete ureteral obstruction. *Lab Invest* 79: 647–658, 1999
33. Bacallao R, Fine LG: Molecular events in the organization of renal tubular epithelium: From nephrogenesis to regeneration. *Am J Physiol* 257: F913–F924, 1989
34. Surendran K, Mccaul SP, Simon TC, A role for Wnt-4 in renal fibrosis. *Am J Physiol* 282: F431–F441, 2002

J Am Soc Nephrol 14: 1427–1434, 2003

The PI3-Kinase-Akt Pathway Promotes Mesangial Cell Survival and Inhibits Apoptosis *In Vitro* via NF-κB and Bad

HARUKO SHIMAMURA, YOSHIO TERADA, TOMOKAZU OKADO, HIROYUKI TANAKA, SEIJI INOSHITA, and SEI SASAKI
The Homeostasis Medicine and Nephrology, Tokyo Medical and Dental University, Tokyo, Japan.

Abstract. While the serine/threonine protein kinase Akt has attracted attention as a mediator of survival (anti-apoptotic) signal, the regulation and function of the PI3-kinase-Akt pathway in mesangial cells is not well known. To explore the significance of the PI3-kinase-Akt pathway, this study used PI3-kinase inhibitors (Wortmannin and LY294002) and recombinant adenoviruses encoding a dominant-active mutant of Akt (AxCAmyrAkt) and a dominant-negative mutant of Akt (AxCAAkt-AA) in cultured rat mesangial cells. Apoptotic signals were measured by nucleosomal laddering of DNA, caspase 3 assay, and cell death detection ELISA. The PI3 kinase inhibitors and dominant-negative mutant of Akt increased the apoptotic signals in the presence of platelet-derived growth factor (PDGF), while the dominant-active mutant of Akt prevented apoptosis induced by a serum-free medium. In separate experiments, we further investigated downstream signals of Akt in mesangial cells. While PDGF activated NF-κB and phosphorylated Bad, these reactions were inhibited by overexpression of the dominant-negative mutant of Akt as well as the PI3-kinase inhibitors. These data indicate, firstly, that Akt is phosphorylated by PDGF, and secondly, that the activated Akt prevents apoptotic changes via activation of NF-κB and phosphorylation of Bad in mesangial cells. This study investigated whether it is Bad phsophorylation or NF-κB activation that provides the anti-apoptotic effects of Akt, and the data suggested that NF-κB is probably the principal contributor to the downstream activation of the PI3-kinase-Akt pathway. The findings suggest that the PI3-kinase-Akt pathway acts as a survival signal and plays a key role in the regulation of apoptotic change in mesangial cells principally via NF-κB.

Akt (also called protein kinase B), the cellular homologue of the v-akt oncogene (1), is a 60-kD serine/threonine kinase cloned by virtue of its homology to PKA and PKC. The kinase is activated in response to stimulation of tyrosine kinase receptors such as platelet-derived growth factor (PDGF), insulin-like growth factor, and nerve growth factor (2–4). The growth factor receptor stimulation of Akt has been shown to be dependent on phosphatidylinositol 3-kinase (PI3-kinase) activity (5–8).

Growing evidence indicates that Akt is a critical mediator of survival signals that protect cells from apoptosis in multiple cell lines (9,10). These studies show that Akt can exert its anti-apoptotic effects in several different ways. For example, phosphorylation of the pro-apoptotic Bad protein by Akt was found to decrease apoptosis by preventing Bad from binding to an anti-apoptotic protein called Bcl-X_L (11,12). Akt was also shown to directly inhibit the activity of a cell death protease caspase-9 (13). Furthermore, Akt is known to promote cell survival by activating nuclear factor-κB (NF-κB), which regulates expression of anti-apoptotic genes (14–16). It should be noted, however, these pathways seem cell-specific, and they are still poorly understood in mesangial cells.

Recent experimental evidence suggests that apoptosis plays pathophysiologic roles in glomerulonephritis. While morphologic evidence of mesangial apoptosis was observed in rat Thy1.1 glomerulonephritis (17–19), the regulation and function of the PI3-kinase-Akt pathway in mesangial cells has not been fully demonstrated under *in vitro* or *in vivo* conditions. To explore the role of the PI3-kinase-Akt pathway, we investigated the regulation of the Akt pathway in cultured mesangial cells in the present study. We demonstrated that anti-apoptotic cell survival pathways help to maintain a balance between cell survival and apoptosis in mesangial cells. In further experiments with the same cell type, we identified that two signal pathways downstream of Akt, namely activation of NF-κB and phosphorylation of Bad, and tried to determine which of them contributed as the anti-apoptotic pathway.

Our results provide insight into the highly organized signaling mechanisms coordinated by the Akt pathway and apoptotic signals in mesangial cells.

Received February 24, 2002. Accepted February 15, 2003.
Correspondence to Dr. Yoshio Terada, Homeostasis Medicine and Nephrology, Tokyo Medical and Dental University, 1-5-45, Yushima, Bunkyo-ku, Tokyo 113-8519, Japan. Phone: 81-3-5803-5214; Fax: 81-3-5803-5215; E-mail: yterada.kid@tmd.ac.jp

1046-6673/1406-1427
Journal of the American Society of Nephrology

DOI: 10.1097/01.ASN.0000066140.99610.32

Materials and Methods

Materials

The specific PI3-kinase inhibitors Wortmannin and LY294002 were purchased from Sigma Chemical (St. Louis, MO). Human PDGF-BB was obtained from Boehringer Mannheim (Mannheim, Germany). RPMI 1640 medium with 2.05 mM L-glutamine was obtained from Iwaki (Chiba, Japan). Acetylsalicylic acid and dexa-

methasone were purchased from Sigma Chemical (St. Louis, MO). A rabbit polyclonal antibody against actin was obtained from Santa Cruz Biotechnology (Santa Cruz, CA).

Recombinant Adenoviruses

Replication-defective, recombinant adenoviruses encoding a dominant active myristoylated Akt (AxCAmyrAkt) and dominant-negative Akt (AxCAAkt-AA) were prepared as described previously. In brief, rat Akt1 was replaced with the myristoylated form (myrAkt) (20). Both Thr308 and Ser473 of rat Akt1 were replaced by alanine (Akt-AA) (21). The recombinant adenovirus expressing the LacZ gene (AxCALacZ) was prepared as described previously (22). Each adenovirus preparation was titrated by plaque-assay on 293 cells. Viral stocks (10^{11} plaque-forming units [pfu]/ml) were stored at −80°C and thawed on ice just before use.

Mesangial Cell Culture

Mesangial cell strains from male Sprague-Dawley rats were isolated and characterized as previously reported (23). The cells were maintained in RPMI1640 medium supplemented with 20% fetal calf serum (FCS), 100 units/ml penicillin, 100 μg/ml streptomycin, 5 μg/ml of insulin, 5 μg/ml of transferrin, and 5 ng/ml selenite at 37°C in a 5% CO_2 incubator. Cells used in experiments were from 5 to10 passages. After an initial incubation in medium plus 20% FCS until approximately 80% confluence, the cells were treated with medium with or without serum, PDGF, LY294002, or Wortmannin for the indicated time and concentration.

Western Blot Analysis

The cell lysates were mixed 1:4 with 5× Laemmli buffer and heated for 5 min at 95°C. Soluble lysates (20 μg) were loaded in each lane and separated by SDS-PAGE using 5% and 20% acrylamide for stacking and resolving gels, respectively. Protein was transferred to nitrocellulose (pore size, 0.45 μm; Schleicher and Schuell, Keene, NH) and probed with polyclonal antibodies against Serine 473-phospho-specific Akt, total-Akt, Serine 136-phospho-specific Bad, total-Bad, and phospho-IκB-α (Ser32; New England Biolabs, Beverly, MA). The primary antibodies (diluted 1/1000) and a second antibody consisting of horseradish peroxidase (HRP)-conjugated goat anti-rabbit IgG (diluted 1/2000; New England Biolabs) were used for the detection of phosphospecific-Akt, total-Akt, phospho-IκB-α (Ser32). The primary antibodies (diluted 1/500 and 1/1000) and a second antibody consisting of HRP-conjugated goat anti-rabbit IgG (diluted 1/2000; New England Biolabs) were used for the detection of phosphospecific-Bad and total-Bad. The bands were visualized by the ECL detection system with 5 to 10 min exposure after extensive washing of the membranes. Controls for protein loading were identified by actin as the internal standard.

Caspase 3and 9 Assays

A Caspase 3 and 9 Fluorometric Protease Assay Kit (MBL, Tokyo, Japan) was used for measurement of caspase 3 and 9 activities as described previously (24). In brief, cells were plated in six-well dishes and cultured in medium of different conditions. The cells were collected and lysed in lysis buffer at indicated times, and the protein concentration was normalized by the Bradford assay. The lysates were incubated with the same amount of reaction buffer and then incubated with 50 μM DEVD-AFC substrate (caspase 3) or 50 μM LEHD-AFC substrate (caspase 9) for 2 h at 37°C. Fluorescence was monitored with an excitation wavelength of 400 nm and an emission wavelength of 505 nm.

Ladder Assays

Adherent and floating cells were collected and lysed in a medium containing 10 mmol/L Tris (pH 8.0), 100 mmol/L NaCl, and 25 mmol/L ethlenediaminetetraacetic acid (EDTA), 0.5% sodium dodecyl sulfate (SDS), and 1.0 mg/ml proteinase K at 37°C for 4 h. DNA was extracted from the digested cells as described previously (25), divided into 30-μg portions, and subjected to electrophoresis on 1.5% agarose gels.

Cell Death ELISA

Histone-associated DNA fragments were quantitated by ELISA (Boerhinger, Mannheim, Germany). All cells from each well were collected by trypsinization and pipetting, pelleted (800 rpm, 5 min), lysed, and subjected to the capture ELISA according to the manufacturer's protocol. Cytosolic proteins were collected using cell lysis buffer according to the manufacturer's protocol. After a 30-min incubation of the cells with cell lysis buffer, the samples were centrifuged for 10 min (15,000 rpm), the nuclei were formed into pellets, the cytoplasmic fraction became supernatant, and the supernatants were collected for the ELISA assay. Each experiment was carried out in triplicate and repeated independently at least five times.

Transient Transfection and Luciferase Assay

Rat mesangial cells were transfected with NF-κB-luciferase-plasmid (NF-κB element × 5 and luciferase fusion plasmid) from Stratagene (La Jolla, CA), and the lysate was used for promoter assay. Data are representative of at least five experiments performed in duplicate. Plasmid DNA (10 μg) were transfected by electroporation method. For experiments performed in exponentially growing cells, luciferase activity was measured 48 h after transfection. Normalization was achieved by cotransfecting 1.0 μg of pCH110, a β-galactosidase reporter construct, as an internal control for the transfection efficiency, as previously reported (26).

Statistical Analyses

The results were given as means ± SEM. The differences were tested using two-way analysis of variance followed by the Scheffe test for multiple comparisons. Two groups were compared by the unpaired *t* test. $P < 0.05$ was considered significant.

Results

Effects of PDGF on Akt Phosphorylation in Cultured Rat Mesangial Cells

To explore the significance of the Akt pathway, we first examined the regulation of the PI3-kinase-Akt pathway in cultured rat mesangial cells. In preliminary experiments, we performed time course of PDGF-induced Akt phosphorylation from 0 to 60 min, the phosphorylation peaked at 15 min. Thus, mesangial cells were exposed to PDGF (5 to 50 ng/ml) for 15 min. Immunoblot analyses for phosphorylation of Akt were performed using phospho-Akt-specific antibody. As shown in Figures 1A and 1B, PDGF treatment increased the Akt phosphorylation dose-dependently, while treatment with the PI3-kinase inhibitor LY294002 (5 μM and 30 μM) reduced it. Similar findings were observed when the cells were pretreated with Wortmannin (20 nM and 50 nM; Figure 1C). These results suggested that Akt is a downstream mediator of PI3-kinase activation in mesangial cells.

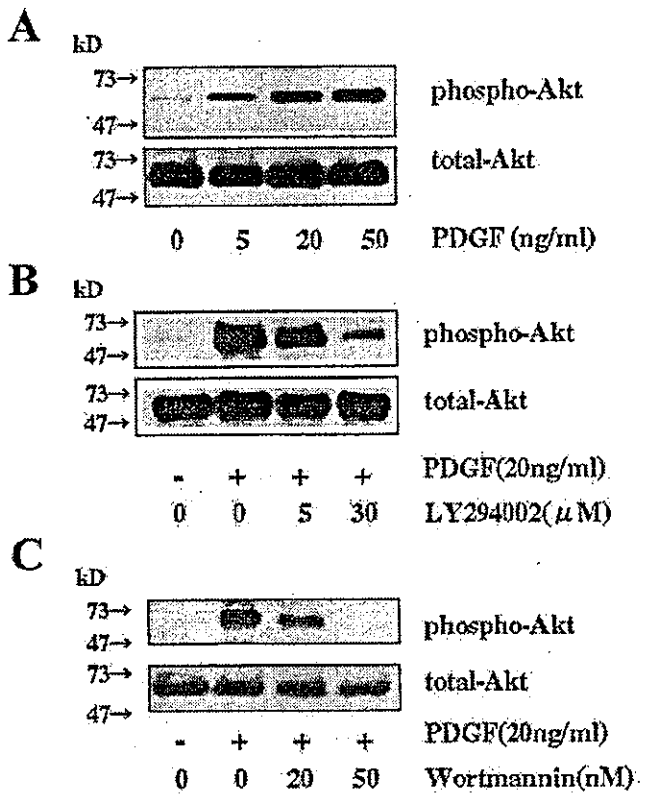

Figure 1. Effect of platelet-derived growth factor (PDGF) on phosphorylation of Akt in cultured rat mesangial cells. (A) PDGF dose-dependently stimulates phosphorylation of Akt in rat mesangial cells. Mesangial cells were incubated with PDGF for 15 min. (B) Inhibition of PDGF-induced phosphorylation of Akt by LY294002 in rat mesangial cells. Mesangial cells were pre-incubated with or without LY294002 for 30 min and then treated with PDGF for 15 min. (C) Inhibition of PDGF-induced phosphorylation of Akt by Wortmannin in rat mesangial cells. Mesangial cells were pre-incubated with or without Wortmannin for 30 min and then treated with PDGF for 15 min. Upper gel, immunoblots using an antibody specific to the phosphorylated form of Akt; lower gel, immunoblots with an antibody to total Akt.

The PI3-Kinase Inhibitors and the Dominant-Negative Mutant of Akt Promoted Apoptosis in PDGF-Treated Mesangial Cells

To investigate the functional roles of the PI3-kinase-Akt pathway, we examined how treatment with PI3-kinase inhibitors (50 nM Wortmannin and 30 μM LY294002) and adenovirus-mediated gene transfer of the dominant-negative mutant of Akt (AxCAAkt-AA) and AxCALacZ (control) influenced the apoptotic phenomena in mesangial cells. Apoptotic signals were measured by nucleosomal laddering of DNA, caspase 3 assay, and cell death detection ELISA. As shown in Figure 2A, the PI3–kinase inhibitors and the dominant-negative mutant of Akt induced nucleosomal laddering of cells in the presence of PDGF. Transfection of AxCAAkt-AA and the PI3–kinase inhibitors also induced caspase 3 activity (Figure 2B). Cell death ELISA examination showed that transfection of AxCAAkt-AA and the PI3-kinase inhibitors significantly increased the apoptotic signals (Figure 2C). According to these results, the inhibition of the PI3- kinase-Akt pathway promoted apoptotic changes in the mesangial cells.

The Dominant-Active Form of Akt Prevented the Induction of Apoptosis by Serum Deprivation in Mesangial Cells

To further examine the functional roles of Akt, we employed adenovirus-mediated gene transfer of the dominant-active mutant of Akt (AxCAmyrAkt) in mesangial cells. Preliminary, we found that apoptotic phenomena such as DNA laddering, increment of caspase 3 activity, and cell death in ELISA assay could be observed in mesangial cells when the cells were incubated in a serum-free condition for 48 h. We then transfected mesangial cells with adenovirus encoding AxCAmyrAkt and AxCALacZ (control) and measured the apoptotic signals. As shown in Figure 3A, the dominant-active mutant of Akt reduced nucleosomal laddering of cells caused by serum withdrawal. Transfection of AxCAmyrAkt also significantly reduced caspase 3 activity (Figure 3B). Cell death ELISA examination showed that the apoptotic signals were significantly inhibited by the transfection of AxCAmyrAkt (Figure 3C). These results demonstrated that the stimulation of the Akt pathway inhibited apoptotic changes induced by serum deprivation in mesangial cells.

Signal Pathways Downstream of Akt in Cultured Rat Mesangial Cells

Several downstream signals of Akt, such as NF-κB, Bad, and caspase 9, have been reported in different cell lines. To examine the signal pathway downstream of Akt in mesangial cells, we began by examining the activation of NF-κB by transfection of NF-κB-luciferase –plasmid (NF-κB element × 5 and luciferase fusion plasmid) and promoter assay. As shown in Figure 4A, the NF-κB luciferase activity stimulated by PDGF was reduced to 35% by a PI3-kinase inhibitor, LY 294002. This stimulation was also reduced to 31% by Wortmannin. In separate experiments using mesangial cells that had been initially transfected with AxCAAkt-AA or AxCALacZ, the NF-κB luciferase activity was reduced to 48% in the AxCAAkt-AA-transfected cells. Noting that NF-κB is held in the cytoplasm as an inactive complex with inhibitor IκB and remains in an inactivate state without IκB phoshorylation, we used Western bolt analysis further evaluate the phoshorylation of IκB with phospho-IκB-specific antibodies. PDGF stimulated the phosphorylation of IκB, and this phosphorylation was inhibited by LY294002, Wortmannin, and transfection of AxCAAkt-AA (Figure 4B). These results suggested that NF-κB is one of the downstream mediators of the PI3-kinase-Akt pathway in mesangial cells.

We next examined whether Bad is associated as a downstream mediator of the PI3-kinase-Akt pathway in cultured rat mesangial cells. Mesangial cells were exposed to PDGF for 20 min. Immunoblot analyses for Bad phosphorylation were performed using phospho-Bad-specific antibody (Ser136). As shown in Figure 5, PDGF treatment increased Bad phosphor-

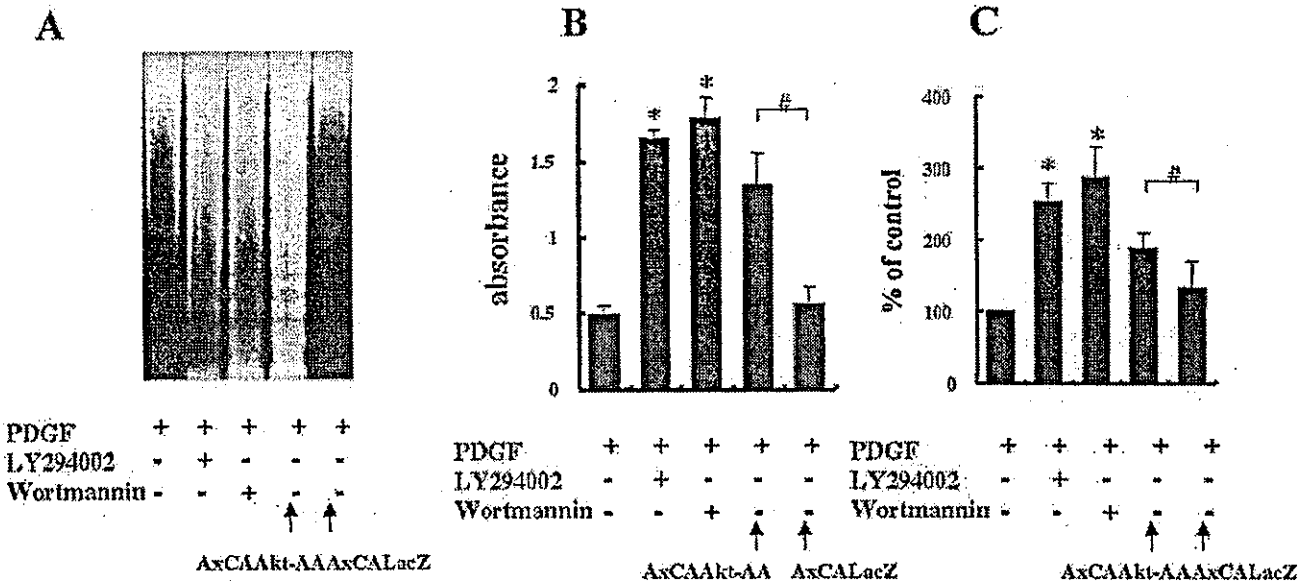

Figure 2. Induction of apoptosis by PI3-kinase inhibitors and dominant-negative Akt in rat mesangial cells. Mesangial cells were initially transfected with AxCAAkt-AA or AxCALacZ for 48 h, incubated with or without PI3-K inhibitors (wortmannin, LY294002) at 30 min before, and then exposed to PDGF for 12 h. (A) Extracted DNA from adherent and floating cells was subjected to electrophoresis on 1.5% agarose gels. (B) Cell lysate was used for caspase 3 assay ($n = 5$, mean ± SEM, $^*P < 0.05$ *versus* PDGF only, $^\#P < 0.05$ AxCALacZ *versus* AxCAAkt-AA). (C) Cell lysate from adherent and floating cells was subjected to cell death ELISA assay ($n = 5$, mean ± SEM, $^*P < 0.05$ *versus* PDGF only; $n = 5$, mean ± SEM, $^\#P < 0.05$ AxCALacZ *versus* AxCAAkt-AA).

ylation and LY294002 (30 μM) inhibited this effect. We performed the same experiments using Wortmannin (50 nM) and obtained similar results. Adenovirus-mediated gene transfer of the dominant-negative mutant of Akt (AxCAAkt-AA) to mesangial cells also reduced the phosphorylation of Bad. These results suggest that Bad is a downstream mediator of the

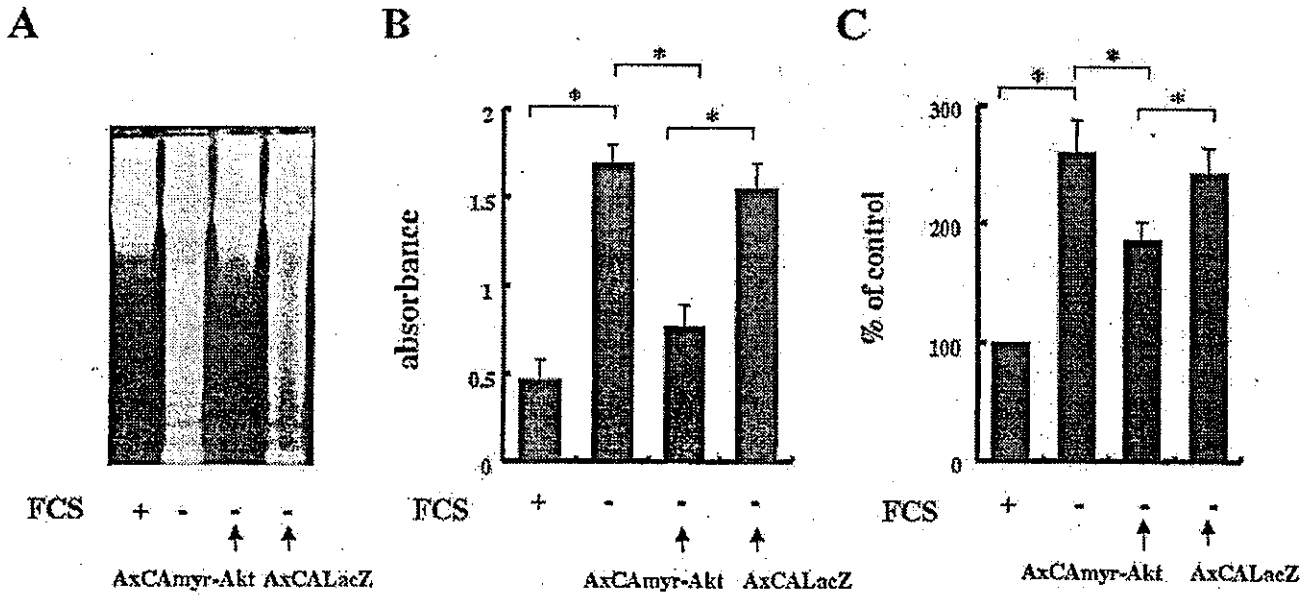

Figure 3. Inhibition of apoptosis by dominant-active Akt in rat mesangial cells. Mesangial cells were transfected with AxCAmyrAkt or AxCALacZ for 48 h and incubated by serum-free medium for 48 h. (A) Extracted DNA from adherent and floating cells was subjected to electrophoresis on 1.5% agarose gels. (B) Cell lysate was used for caspase 3 assay ($n = 5$, mean ± SEM, $^*P < 0.05$). (C) Cell lysate from adherent and floating cells was subjected to cell death ELISA assay ($n = 5$, mean ± SEM, $^*P < 0.05$).

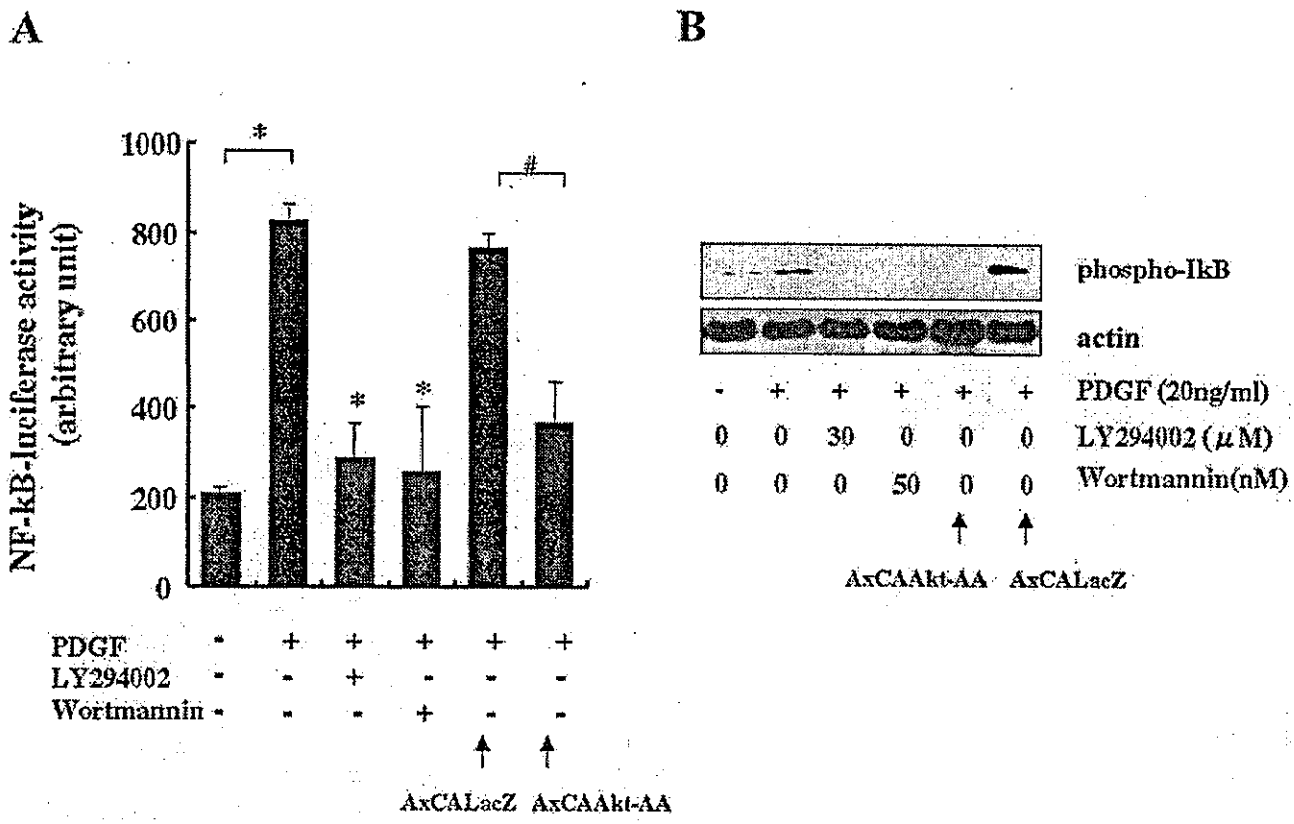

Figure 4. Effect of PDGF on nuclear factor-κB (NF-κB) luciferase activity and phosphorylation of IκB in cultured rat mesangial cells. (A) Mesangial cells were initially transfected with NF-κB luciferase plasmid, and then transfected AxCAAkt-AA or AxCALacZ for 48 h, or incubated with or without PI3-kinase inhibitors (Wortmannin, LY294002) for 30 min. The cells were exposed to PDGF for 6 h and harvested for luciferase assay. ($n = 5$, mean ± SEM, $^*P < 0.05$ *versus* PDGF only; $^\#P < 0.05$ AxCALacZ *versus* AxCAAkt-AA). (B) Mesangial cells were incubated with PDGF for 30 min. Phosphorylation of IκB in cultured rat mesangial cells was detected by immunoblots using an antibody specific to the phosphorylated form of IκB. Inhibition of PDGF-induced phosphorylation of IκB by LY294002 and Wortmannin in rat mesangial cells. Mesangial cells were pre-incubated with or without LY294002 or Wortmannin for 30 min and then treated with PDGF for 30 min. Mesangial cells were transfected with AxCAAkt-AA or AxCALacZ for 48 h and then treated with PDGF for 30 min. Upper gel, immunoblots using an antibody specific to the phosphorylated form of IκB; lower gel, immunoblots with an antibody to actin.

PI3-kinase activation in mesangial cells. In further experiments, we examined whether inhibition of Akt phosphorylaion by LY294002, Wortmannin, and the dominant-negative mutant of Akt (AxCAAkt-AA) altered the activity of caspase 9. As shown in Figure 6, caspase 9 activity was higher in the condition without serum. Caspase 9 activity was increased in mesangial cells cultured with PDGF alone than it was in cells cultured with FCS. We used this pro-apoptotic condition in the following experiments. In the experiments using transfected AxCAAkt-AA and PI3–kinase inhibitors, caspase 9 activity was not significantly changed from the activity observed in the presence of PDGF alone at neither 12 h nor 24 h (Figure 6 shows at 12 h). Thus, the Akt pathway seemed to play only a minor role in caspase 9 activity under our experimental condition. Judging from these data, there are at least two signaling pathways (via NF-κB and Bad) downstream of the PI3-kinase-Akt pathway in mesangial cells.

Next, we tried to assess the relative contributions of Bad and NF-κB signaling downstream of the PI3-kinase-Akt pathway to determine which plays a principal role. Our first step was to examine the effects of the NF-κB inhibitors (acetylsalicylic acid [ASA] and dexamethasone [Dex]). As shown in Figure 7, PDGF stimulated the phosphorylation of IκB, and this phosphorylation was dose-dependently inhibited by ASA and Dex. We next examined the apoptotic signal. As shown in Figure 7C, the transfection of AxCAmyrAkt significantly reduced caspase 3 activity, but this attenuating effect was abolished in the cells treated with ASA and Dex. These results demonstrated that NF-κB activation was essential for the prevention of apoptotic change in the Akt pathway.

We also examined the time course of Bad and IκB phosphorylation. In the assessment of Bad phosphorylation, the Bad stayed phosphorylated for 3 h after the PDGF stimulation (Figure 8A). The IκB phosphorylation appeared at 30 min after PDGF stimulation and lasted for 12 h (Figure 8B). As shown in Figure 8C, the Akt phosphorylation appeared at 10 min after PDGF stimulation and Akt stayed phosphorylated for 12 h. Since there was no way to directly inhibit Bad phoshorylation,

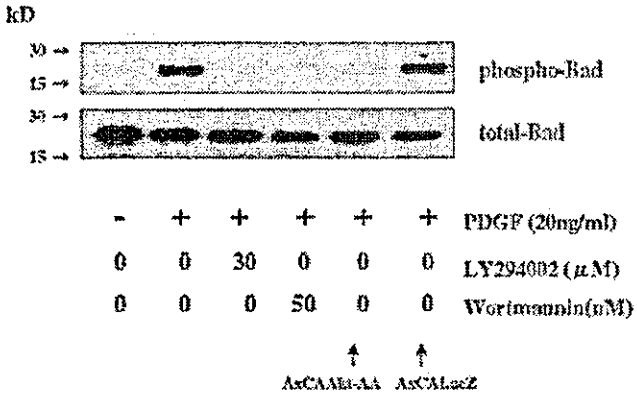

Figure 5. Effect of PDGF on phosphorylation of Bad in cultured rat mesangial cells. Mesangial cells were pre-incubated with or without LY294002 or Wortmannin for 30 min and then treated with PDGF for 20 min. Mesangial cells were transfected with AxCAAkt-AA or AxCALacZ for 48 h, and then treated with PDGF for 20 min. Upper gel, immunoblots using an antibody specific to the phosphorylated form of Bad; lower gel, immunoblots with an antibody to total Bad.

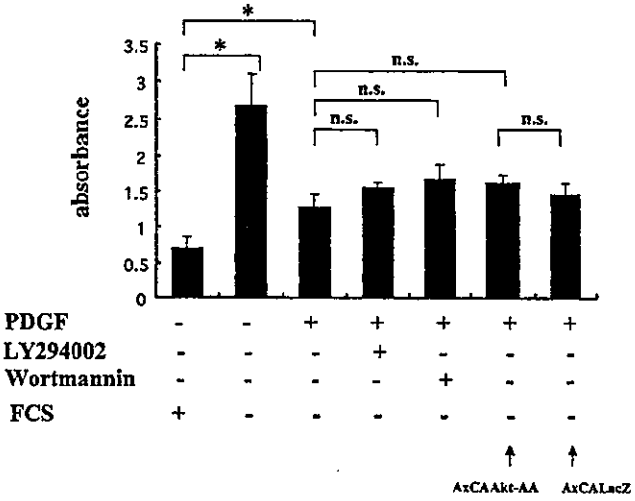

Figure 6. Induction of caspase 9 by PI3-kinase inhibitors and dominant-negative Akt in rat mesangial cells. Mesangial cells were transfected with either AxCAAkt-AA or AxCALacZ for 48 h, incubated with or without PI3-kinase inhibitors (Wortmannin, LY294002) for 30 min, and then immediately exposed to PDGF for 12 h. All cell lanes were treated with FCS-free medium except the lane of FCS(+). Cell lysate was used for caspase 9 assay ($n = 6$, mean ± SEM, $^*P < 0.05$).

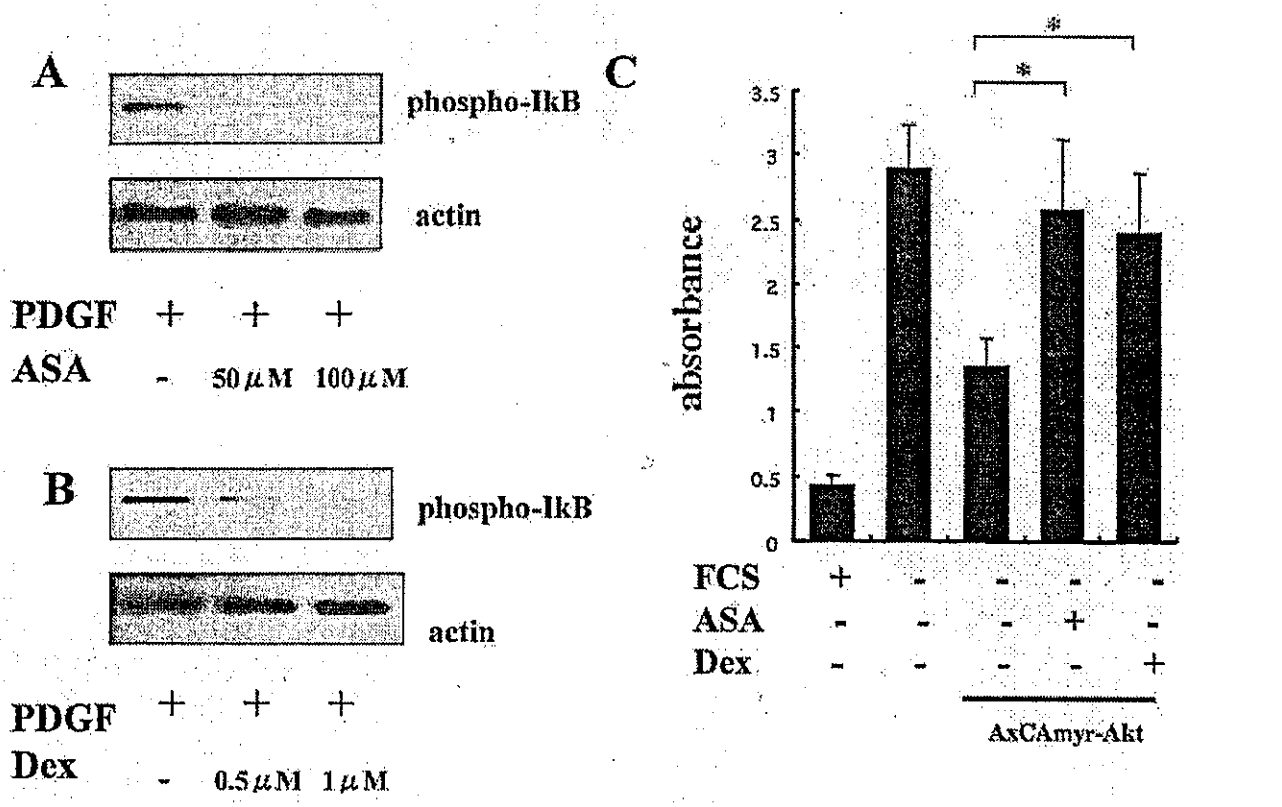

Figure 7. Inhibition of PDGF-induced phosphorylation of Akt by NF-κB inhibitors in rat mesangial cells. (A) Mesangial cells were incubated with PDGF (20 μg/ml) in the presence or absence of acetylsalicylic acid (ASA) for 30 min. (B) Mesangial cells were incubated with PDGF (20 μg/ml) and in the presence or absence of dexamethasone (Dex) for 30 min. (C) Mesangial cells were transfected with AxCAmyrAkt or AxCALacZ for 48 h, incubated in serum-free medium for 48 h, and then incubated with or without NF-κB inhibitors (ASA, 50 μM; Dex, 0.5 μM). Cell lysate was used for caspase 3 assay ($n = 5$, mean ± SEM, $^*P < 0.05$).

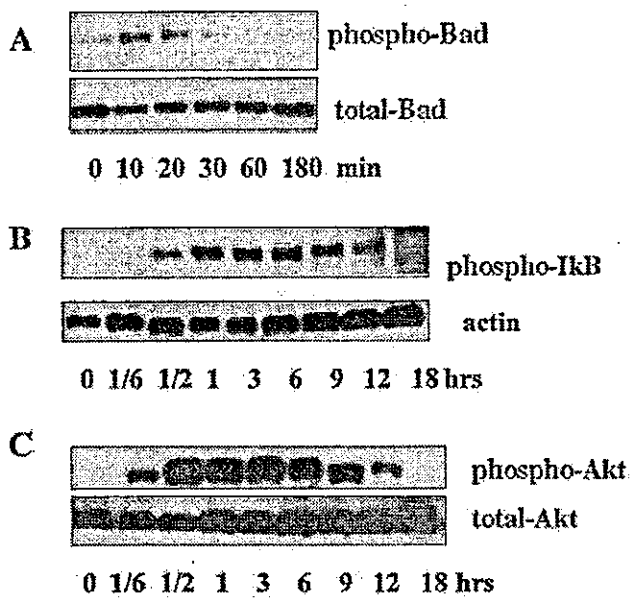

Figure 8. Time courses of phosphorylation of Bad, IκB, and Akt. Rat mesangial cells were incubated with PDGF (20 μg/ml) for the indicated periods. (A) Upper gel, immunoblots using an antibody specific to the phosphorylated form of Bad; lower gel, immunoblots with an antibody to total Bad. (B) Upper gel, immunoblots using an antibody specific to the phosphorylated form of IκB; lower gel, immunoblots with an antibody to actin. (C) Upper gel, immunoblots using an antibody specific to the phosphorylated form of Akt; lower gel, immunoblots with an antibody to total Akt.

we could not make any comparison by inhibiting the pathway. However, the longstanding activation of NF-κB up to the appearance of the apopototic changes and the effect of NF-κB in abolishing the anti-apoptotic effect of Akt, both suggest that NF-κB could be a dominant pathway in rat mesangial cells.

Discussion

In the present study, we demonstrated that Akt is phosphorylated by PDGF and that activated Akt prevents apoptotic changes in rat mesangial cells. In addition, we characterized the downstream signals of the PI3-kinase-Akt pathway. Our *in vitro* data suggest that this pathway acts as a survival signal and plays a key role in the regulation of apoptotic change in mesangial cells.

In this study, we demonstrated that the PI3-kinase-Akt pathway is activated by PDGF in mesangial cells. PDGF is known to be a potent mediator in the proliferation of mesangial cells, and the MAP kinase and the JAK-STAT pathway have been reported to be involved in this PDGF-mediated signaling cascade (27,28). PDGF drives the mesangial cell proliferation in many progressive renal diseases (6). A recent investigation showed that Akt promotes mesangial cell proliferation via inhibition of $P27^{kip1}$ transcription in mesangial cells (29). PDGF is also to be a principal survival factor that inhibits apoptosis and promotes proliferation in several cell types. In this report, we demonstrated that the PI3-kinase-Akt pathway acts as a survival (anti-apoptotic) signal and that PDGF activates that pathway in mesangial cells. While PDGF has been reported to mediate the proliferation that deeply involved in the mesangial proliferation of Thy 1.1 nephritis and IgA nephritis (17–19), our data suggest that PDGF serves a separate function as a survival factor acting through the PI3-kinase-Akt pathway in glomerulonephritis.

Several targets of Akt survival signal have been identified in different cell types. Among them, the NF-κB protein has been shown to promote expression of anti-apoptotic genes. Recent reports demonstrated a direct association between Akt and phosphorylation of IκB in fibroblasts by identifying NF-κB as a target of Akt in anti-apoptotic PDGF signaling (14,15,30,31). In contrast, other investigators working with human vascular smooth muscle cells and skin fibroblasts concluded that Akt phosphorylation and NF-κB activation share no association (32). Thus, it remains controversial whether NF-κB is indeed involved in the PI3-kinase-Akt. Our data identified that NF-κB as a downstream mediator of the PI3-kinase-Akt pathway in mesangial cells.

We also demonstrated that Bad is phosphorylated by Akt in mesangial cells. Bad is a proapoptotic protein form of the Bcl-2 family members. Phosphorylation of Bad promotes cell survival in many cell types, and several reports have suggested that Bad is a downstream signal of the Akt pathway. In neurons, growth factor activation of the PI3-kinase-Akt pathway stimulates the phosphorylation of Bad, thereby suppressing apoptosis and promoting cell survival. Phosphorylation of Bad at Ser-136 by activated Akt results in its dissociation from Bcl-X_L and association with the adapter protein 14-3-3 (12). The free Bcl-X_L released from sequestration by Bad promotes cell survival. Our data indicate that part of the anti-apoptotic action of the PI3-kinase-Akt pathway is elicited via phosphorylation of Bad in mesangial cells.

A previous report suggested that the phosphorylation of Akt directly suppresses caspase 9 activity and inhibits apoptosis in human umbilical endothelial cells (14). When we attempted to examine whether the inhibition of Akt phosphorylaion would alter the activity of caspase 9, no significant difference was observed under our experimental condition. Taken together, these results imply that NF-κB and Bad are both involved in the signal pathway downstream of the PI3-kinase-Akt-pathway in mesangial cells.

The remaining question is which of these, NF-κB or Bad, acts as the principal signaler downstream of the PI3-kinase-Akt pathway. As we mentioned above, the Akt-induced activation of NF-κB and phosphorylation of Bad both seem to be cell-specific events. For two reasons, our data suggested that NF-κB contributes more as a downstream signaler in rat mesangial cells: NF-κB was still activated by the time the apopototic changes were observed, and inhibition of NF-κB activation reduced the anti-apoptotic effect of dominant-active Akt.

In summary, we investigated the regulation and function of the PI3-kinase-Akt pathway and the downstream signal of Akt in cultured rat mesangial cells. Our findings indicate that Akt is phosphorylated by PDGF and that the activated Akt prevents apoptotic changes partly via the downstream signaling of

NF-κB and Bad. In our data characterizing the relative contributions of NF-κB and Bad to this pathway, the former seemed to contribute more. These results suggest that the PI3-kinase-Akt pathway acts as a survival signal and plays a key role in the regulation of apoptotic change in mesangial cells.

Acknowledgments

We are grateful to Dr. Wataru Ogawa and Dr. Masato Kasuga for providing the recombinant adenoviruses encoding a dominant active myristoylated Akt (AxCAmyrAkt) and dominant-negative Akt (AxCAAkt-AA).

References

1. Datta SR, Brunet A, Greenberg ME: Cellular survival: A play in three Akts. *Genes* 13: 2905–2927, 1999
2. Datta K, Franke TF, Chan TO, Makris A, Yang SI, Kaplan DR, Morrison DK, Golemis EA, Tsichlis PN: AH/PH domain-mediated interaction between Akt molecules and its potential role in Akt regulation. *Mol Cell Biol* 15: 2304–2310, 1995
3. Kulik G, Klippel A, Weber MJ: Antiapoptotic signalling by the insulin-like growth factor I receptor, phosphatidylinositol 3-kinase, and Akt. *Mol Cell Biol* 17: 1595–1606, 1997
4. Yao R, Cooper GM: Requirement for phosphatidylinositol-3 kinase in the prevention of apoptosis by nerve growth factor. *Science* 267: 2003–2006, 1995
5. Fruman DA, Meyers RE, Cantley LC: Phosphoinositide kinases. *Annu Rev Biochem* 67: 481–507, 1998
6. Choudhury GG, Karamitsos C, Hernandez J, Gentilini A, Bardgette J, Abboud HE: PI-3-kinase and MAPK regulate mesangial cell proliferation and migration in response to PDGF. *Am J Physiol* 273: F931–938, 1997
7. Franke TF, Yang SI, Chan TO, Datta K, Kazlauskas A, Morrison DK, Kaplan DR, Tsichlis PN: The protein kinase encoded by the Akt proto-oncogene is a target of the PDGF-activated phosphatidylinositol 3-kinase. *Cell* 81: 727–736, 1995
8. Franke TF, Kaplan DR, Cantley LC: PI3K: downstream AKTion blocks apoptosis. *Cell* 88: 435–437, 1997
9. Brunet A, Bonni A, Zigmond MJ, Lin MZ, Juo P, Hu LS, Anderson MJ, Arden KC, Blenis J, Greenberg ME: Akt promotes cell survival by phosphorylating and inhibiting a Forkhead transcription factor. *Cell* 96: 857–868, 1999
10. Downward J: Mechanisms and consequences of activation of protein kinase B/Akt. *Curr Opin Cell Biol* 10: 262–267, 1998
11. Dudek H, Datta SR, Franke TF, Birnbaum MJ, Yao R, Cooper GM, Segal RA, Kaplan DR, Greenberg ME: Regulation of neuronal survival by the serine-threonine protein kinase Akt. *Science* 275: 661–665, 1997
12. Datta SR, Dudek H, Tao X, Masters S, Fu H, Gotoh Y, Greenberg ME: Akt phosphorylation of BAD couples survival signals to the cell-intrinsic death machinery. *Cell* 91: 231–241, 1997
13. Kennedy SG, Kandel ES, Cross TK, Hay N: Akt/Protein kinase B inhibits cell death by preventing the release of cytochrome c from mitochondria. *Mol Cell Biol* 19: 5800–5810, 1999
14. Cardone MH, Roy N, Stennicke HR, Salvesen GS, Franke TF, Stanbridge E, Frisch S, Reed JC: Regulation of cell death protease caspase-9 by phosphorylation. *Science* 282: 1318–1321, 1998
15. Khwaja A: Akt is more than just a Bad kinase. *Nature* 401: 33–34, 1999
16. Ozes ON, Mayo LD, Gustin JA, Pfeffer SR, Pfeffer LM, Donner DB: NF-κB activation by tumour necrosis factor requires the Akt serine-threonine kinase. *Nature* 401: 82–85, 1999
17. Shimizu A, Kitamura H, Masuda Y, Ishizaki M, Sugisaki Y, Yamanaka N: Apoptosis in the repair process of experimental proliferative glomerulonephritis. *Kidney Int.* 47: 114–121, 1995
18. Harrison DJ: Cell death in the diseased glomerulus. *Histopathology* 12: 679–683, 1988
19. Sugiyama H, Kashihara N, Makino H, Yamasaki Y, Ota A: Apoptosis in glomerular sclerosis. *Kidney Int* 49: 103–111, 1988
20. Kitamura T, Ogawa W, Sakaue H, Hino Y, Kuroda S, Takata M, Matsumoto M, Maeda T, Konishi H, Kikkawa U, Kasuga M: Requirement for activation of the serine-threonine kinase Akt (protein kinase B) in insulin stimulation of protein synthesis but not of glucose transport. *Mol Cell Biol* 18: 3708–3717, 1998
21. Kotani K, Ogawa W, Hino Y, Kitamura T, Ueno H, Sano W, Sutherland C, Granner DK, Kasuga M: Dominant negative forms of Akt (protein kinase B) and atypical protein kinase Clambda do not prevent insulin inhibition of phosphoenolpyruvate carboxykinase gene transcription. *J Biol Chem* 274: 21305–21312, 1999
22. Terada Y, Yamada T, Nakashima O, Tamamori M, Ito H, Sasaki S, Marumo F: Overexpression of cell cycle inhibitors (p16INK4 and p21Cip1) and cyclin D1 using adenovirus vectors regulates proliferation of rat mesangial cells. *J Am Soc Nephrol* 8: 51–60, 1997
23. Owada A, Tomita K, Terada Y, Sakamoto H, Nonoguchi H, Marumo F: Endothelin (ET)-3 stimulates cyclic guanosine 3', 5'-monophosphate production via ETB receptor by producing nitric oxide in isolated rat glomerulus, and in cultured rat mesangial cells. *J Clin Invest* 93: 556–563, 1994
24. Inoshita S, Terada Y, Nakashima O, Kuwahara M, Sasaki S, Marumo F: Roles of E2F1 in mesangial cell proliferation in vitro. *Kidney Int* 56: 2085–2095, 1999
25. Terada Y, Inoshita S, Hanada S, Shimamura H, Kuwahara M, Ogawa W, Kasuga M, Sasaki S, Marumo F: Hyperosmolality activates Akt and regulates apoptosis in renal tubular cells. *Kidney Int* 60: 553–567, 2001
26. Terada Y, Nakashima O, Inoshita S, Kuwahara M, Sasaki S, Marumo F: TGF-beta-activating kinase-1 inhibits cell cycle and expression of cyclin D1 and A in LLC-PK1 cells. *Kidney Int* 56: 1378–1390, 1999
27. Dudley DT, Pang L, Decker SJ, Bridges AJ, Saltiel AR: A synthetic inhibitor of the mitogen-activated protein kinase cascade. *Proc Natl Acad Sci USA* 92: 7686–7689, 1995
28. Potts JD, Kornacker S, Beebe DC: Activation of the Jak-STAT-signaling pathway in embryonic lens cells. *Dev Biol* 204: 277–292, 1998
29. Choudhury GG: Akt serine threonine kinase regulates platelet-derived growth factor-induced DNA synthesis in glomerular mesangial cells: regulation of c-fos AND p27(kip1) gene expression. *J Biol Chem* 276: 35636–35643, 2001
30. Romashkova JA, Makarov SS: NF-κB is a target of AKT in anti-apoptotic PDGF signalling. *Nature* 401: 86–90, 1999
31. Maehara K, Oh-Hashi K, Isobe KI: Early growth-responsive-1-dependent manganese superoxide dismutase gene transcription mediated by platelet-derived growth factor. *FASEB J* 15: 2025–2026, 2001
32. Rauch BH, Weber A, Braun M, Zimmermann N, Schror K: PDGF-induced Akt phosphorylation does not activate NF-kappa B in human vascular smooth muscle cells and fibroblasts. *FEBS Lett* 481: 3–7, 2000

J Am Soc Nephrol 14: 3090–3101, 2003

Leukemia Inhibitory Factor Is Involved in Tubular Regeneration after Experimental Acute Renal Failure

JUN YOSHINO, TOSHIAKI MONKAWA, MIHOKO TSUJI, MATSUHIKO HAYASHI, and TAKAO SARUTA
Department of Internal Medicine, School of Medicine, Keio University, Tokyo, Japan.

Abstract. Leukemia inhibitory factor (LIF) is known to play a crucial role in the conversion of mesenchyme into epithelium during nephrogenesis. This study was carried out to test the hypothesis that LIF and LIF receptor (LIFR) are involved in the renal epithelial regeneration after acute renal failure. First, the authors investigated the spatiotemporal expression of LIF and LIFR in fetal and adult rat kidney. In developing kidney, LIF was expressed in the ureteric buds and LIFR was located in nephrogenic mesenchyme and the ureteric buds; in adult kidney, LIF and LIFR expression was confined to the collecting ducts. Next, the authors examined the expression of LIF and LIFR during the recovery phase after ischemia-reperfusion injury. Real-time PCR analysis revealed that LIF mRNA expression was significantly increased from day 1 to day 7 after reperfusion and that LIFR mRNA was upregulated from day 4 to day 14. Histologic analysis demonstrated that the increased expression of LIF mRNA and protein was most marked in the outer medulla, especially in the S3 segment of the proximal tubules. To elucidate the mitogenic role of LIF in the regeneration process, cultured rat renal epithelial (NRK 52E) cells were subjected to ATP depletion (an *in vitro* model of acute renal failure), and LIF expression was found to be enhanced during recovery after ATP depletion. Blockade of endogenous LIF with a neutralizing antibody significantly reduced the cell number and DNA synthesis during the recovery period. These results suggest that LIF participates in the regeneration process after tubular injury.

The mammalian kidney is susceptible to injury by ischemia and nephrotoxins, and recovery of normal renal function requires regeneration of damaged tubular epithelium. The process of regeneration after renal injury is characterized by a sequence of events that includes epithelial cell spreading, migration to cover exposed areas of the basement membrane, cell dedifferentiation and proliferation to restore cell number, and then differentiation (1,2). In many respects this nephrogenic repair process resembles the growth and maturation of nephrons during kidney development (3,4). Several genes critical for kidney development have been shown to be upregulated in the regeneration process after injury and participate in the regeneration. Pax-2 (5), Wnt-4 (6), and activin-A (7) have been shown to be re-expressed in the regenerating tubules after injury (8–11). These findings support the hypothesis that a cascade of developmental gene pathways is reactivated during tissue regeneration.

Leukemia inhibitory factor (LIF), a member of the interleukin-6 (IL-6) family, is a multifunctional cytokine originally identified as a proliferation inhibitor and differentiation inducer of mouse myeloid leukemia cell line M1 (12,13). LIF is synthesized by a variety of cells, including renal epithelial cells (14), and, functionally, it has been implicated in a number of processes including development, hematopoiesis, inflammation, and regeneration after injury (15). LIF has been shown to play a pivotal role in kidney development. It is secreted by ureteric buds and induces conversion of mesenchyme into epithelium (16).

The importance of LIF in nephrogenesis prompted us to test the hypothesis that LIF participates in renal epithelial tubular regeneration. In this study, we first investigated the expression of LIF and LIF receptor (LIFR) in ischemia/reperfusion–injured kidney and in normal fetal and adult rat kidney; we then used an *in vitro* ischemia model (ATP depletion method) to investigate the mitogenic effect of LIF on kidney epithelial cells (NRK 52E) during the regenerative process. The results showed that LIF is transiently increased in regenerating tubular cells during the recovery phase both *in vivo* and *in vitro* and that LIF contributes to renal epithelial regeneration.

Materials and Methods

Animals

Sprague-Dawley rats were obtained from Charles River Japan (Tokyo, Japan) and anesthetized by intraperitoneal injection of pentobarbital before use in the experiments. All procedures employed in the animal experiments were conducted in accordance with the Guideline for the Care and Use of Laboratory Animals of Keio University School of Medicine.

Bilateral ischemic renal injury was produced in male rats weighing 200 to 230 g by clamping both renal arteries for 45 min. The clamp

Received August 8, 2003. Accepted September 21, 2003.
Correspondence to Dr. Toshiaki Monkawa, Department of Internal Medicine, School of Medicine, Keio University, 35 Shinanomachi, Shinjuku-ku, Tokyo 160–8582, Japan. Phone: 81-3-5363-3796; Fax: 81-3-3359-2745; E-mail: monkawa@sc.itc.keio.ac.jp
1046-6673/1412-3090
Journal of the American Society of Nephrology

DOI: 10.1097/01.ASN.0000101180.96787.02

was then removed to allow reperfusion, and rats were killed after 1, 2, 4, 7, 14, and 30 d of reperfusion ($n = 5$ or 6 per group).

For histologic assessment, fetal and adult kidneys were fixed in 10% phosphate-buffered formalin, embedded in paraffin, and cut serially into 5-μm-thick sections.

Real-Time PCR

Total RNA was isolated from kidney homogenates and cultured cells with the TRIzol Reagent (Invitrogen, Carlsbad, CA). First-strand cDNA was synthesized from total RNA by using random hexamers. Real-time PCR was performed on a TaqMan ABI 7700 Sequence Detection System (Applied Biosystems, Foster City, CA). PCR amplification was performed using TaqMan PCR Universal Master Mix (Applied Biosystems). Thermal cycler conditions consisted of holding at 50°C for 2 min and 95°C for 10 min, followed by 30–40 cycles of 95°C for 15 s and 60°C for 1 min. The following oligonucleotide primers (50 nM) and probes (200 nM) were used: rat LIF (GenBank accession number AB010275): sense, 5'-CAGTGCCAATGCCCTCTTTA-3', antisense, 5'-GCATGGAAAGGTGGGAAATC-3'; internal fluorescence-labeled TaqMan MGB probe (FAM): 5'-CCCAACAACGTGGATAAGCTATGTGCGC-3'; rat LIF receptor (GenBank accession number D86345): sense, 5'- TCATCAGTGTGGTGGCAAGAA-3', antisense, 5'- TCATCAGTGTGGTGGCAAGAA-3'; internal fluorescence-labeled TaqMan probe (FAM): 5'-TTCTGCCGGTTCATCTCCACCTTCAA-3'. Gene expression of the target sequence was normalized in relation to expression of 18S ribosomal RNA as an endogenous control. Each sample was tested in duplicate. Results are expressed relative to data from pre-ischemic kidneys that were arbitrarily assigned a value of 1.

In Situ *Hybridization*

A cDNA for rat LIF was generated by reverse transcription-PCR with the following primers: sense, 5'-TGCCCCTACTGCTCATTCTG-3', antisense, 5'-GACACAGGGCACATCCACAT-3'. The amplified PCR fragment was initially ligated to pCR II vector (Invitrogen) and digoxigenin (DIG)–labeled antisense, and sense cRNA probes were synthesized with T7 or SP6 RNA polymerases (DIG RNA labeling kit SP6/T7; Roche Diagnostics, Indianapolis, IN). Tissue sections were deparaffinized, permeablized with proteinase K, and refixed with 4% paraformaldehyde in phosphate-buffered saline (PBS). The prehybridization and hybridization steps were carried out at 65°C for 2 h and 12 h, respectively. The hybridization buffer was composed of 50% formamide, 5 × SSC, 5 × Denhardt's solution, 250 μg/ml Baker's yeast tRNA, 500 μg/ml salmon sperm DNA, and cRNA probes. After post-hybridization washing, sections were incubated with anti-digoxigenin antiserum conjugated to alkaline phosphatase, and histochemical detection was performed using a 4-nitroblue tetrazolium chloride/5-bromo-4-chloro-3-indolyl-phosphate mixture (Roche Diagnostics). The same procedure performed with the sense cRNA probe served as a negative control.

Immunohistochemical Staining

After deparaffinization, sections were treated with 0.3% hydrogen peroxidase in methanol for 30 min to remove endogenous peroxidase activity. They were then blocked in normal horse serum and incubated at 4°C overnight with the primary antibodies: anti-mouse LIF antibody (R&D Systems, Minneapolis, MN), anti-human LIFR antibody (Santa Cruz Biotechnology, Santa Cruz, CA), and anti-human aquaporin-1 (AQP-1) antibody (Alomone Labs, Jerusalem, Israel). Next, the sections were incubated with biotinylated secondary antibody and incubated with avidin-biotin horseradish peroxidase complex (Vectastain Elite ABC kit; Vector Laboratories, Burlingame, CA). The sections were visualized with a Vector DAB peroxidase substrate kit (Vector Laboratories) and were counterstained with hematoxylin. As a negative control, the primary antibody was replaced with normal horse serum, and no positive immunostaining was observed.

For 5-bromo-2'-deoxyuridine (BrdU) staining, rats were intraperitoneally injected with BrdU 2 h before sacrifice. Formalin-fixed paraffin sections were subjected to BrdU staining by using a Cell Proliferation Kit (Amersham Biosciences, Piscataway, NJ) according to the manufacturer's instructions. In brief, after deparaffinization, sections were treated with 0.3% hydrogen peroxidase in methanol for 30 min to remove endogenous peroxidase activity. Tissue sections were then placed in citrate buffer and heated for 10 min in a microwave oven; after incubating them with anti-BrdU antibody, the sections were incubated with HRP-conjugated IgG and developed with a Vector DAB peroxidase substrate kit.

Double immunohistochemistry was performed to detect LIF expression in combination with the proximal tubular marker AQP-1 (17,18). The first immunohistochemical staining was performed with a Vector VIP substrate kit (Vector Laboratories) to obtain a purple reaction product, and the sections were then washed and blocked with an avidin-biotin blocking kit (Vector Laboratories). The second immunostaining was performed with a Vector SG substrate kit (Vector Laboratories) to obtain a blue reaction product.

Cell Culture

A normal rat kidney epithelial-derived cell line, NRK 52E (19), was grown in Dulbecco modified essential medium with 10% fetal bovine serum, 100 U/ml penicillin, and 100 U/ml streptomycin, in a humidified 5% CO_2/95% air environment at 37°C.

ATP Depletion Protocol

ATP depletion of NRK 52E cells was achieved by means of previously described protocols with modifications (20,21). A confluent monolayer of NRK 52E cells was incubated in PBS with 1.5 mM $CaCl_2$, 2 mM $MgCl_2$, and 1 μM antimycin A (Sigma, St. Louis, MO) for 60 min. During the recovery phase after the 1-h injury period, cells were repleted with ATP by incubation with a regular growth medium. Cellular ATP levels were determined with a luciferase-based assay kit (Sigma).

Effect of LIF Antibody on Cell Proliferation

NRK 52E cells were subcultured in 24-well plates for cell counting, or in 96-well plates for measurement of BrdU incorporation, and subjected to ATP depletion for 1 h as described above. After the injury, cells were repleted with ATP by incubation with recovery medium containing affinity-purified anti-human LIF antibody (Genzyme, Cambridge, MA) at the concentration indicated, or with normal goat IgG as a negative control. The number of living cells was counted with a Cell Counting Kit-8 (Wako Pure Chemicals, Osaka, Japan) after the 48-h recovery phase ($n = 4$). DNA synthesis was assessed by an enzyme-linked immunosorbent assay for BrdU (Roche Diagnostics) after the 24-h recovery phase ($n = 6$).

Statistical Analyses

Statistical significance was evaluated by one-way ANOVA with a Fisher's post-hoc test. Statistical significance was defined as $P < 0.05$.

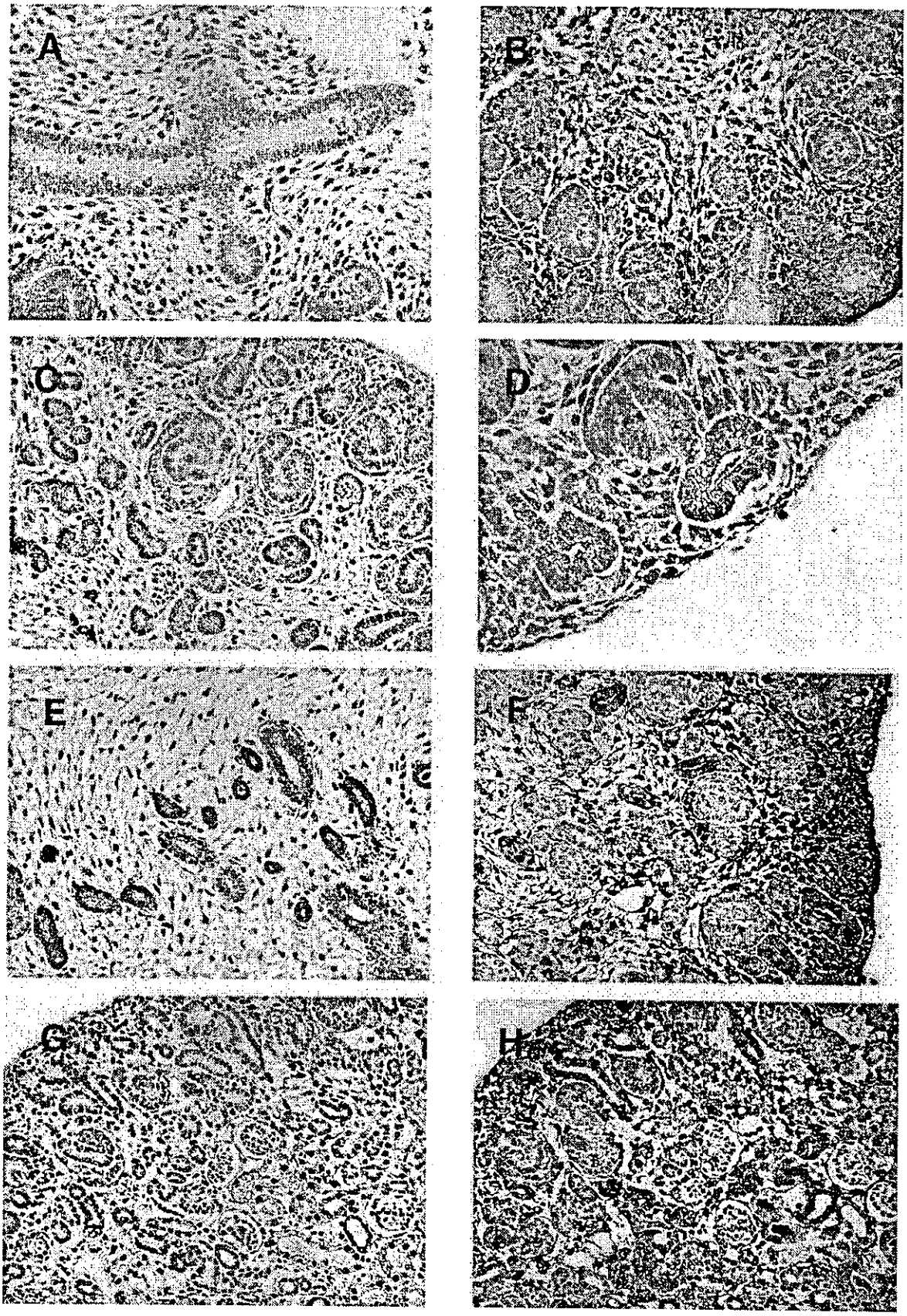
A
B
C
D
E
F
G
H

Results

Localization of LIF and Its Receptor in Developing and Adult Rat Kidneys

The spatiotemporal expression of LIF and LIFR during kidney development was investigated by an immunohistochemical technique. At embryonic day 15 (E15), LIF expression level was very low (Figure 1A). Weak LIF immunoreactivity was observed in the ureteric buds, whereas LIFR immunoreactivity was observed in the mesenchymal cells surrounding the ureteric buds (Figure 1B). At E17, LIF immunostaining was noted in derivatives of the ureteric buds, whereas no immunostaining was detected in the mesenchymal cells (Figure 1C). In the nephrogenic outer cortex, LIF was expressed in the tips of the branches of the ureteric buds (Figure 1D); in the medulla, intense staining was found in the major branches of the ureteric buds and collecting ducts (Figure 1E). At E17, LIFR was expressed ubiquitously in mesenchyme, and the most intense signal was observed in the condensing mesenchymal cells surrounding the tips of the ureteric buds in the nephrogenic zone (Figure 1F). In addition to the mesenchymal cells, the derivatives of the ureteric buds, including ureteric bud branch tips and collecting ducts, expressed LIFR, a pattern that resembled the distribution of LIF protein observed. The ureteric buds differentiated into collecting ducts, as nephrogenesis progressed. In neonatal kidneys, LIF was expressed predominantly in mature and immature collecting ducts (Figure 1G). LIFR was also expressed in mature and immature collecting ducts, whereas LIFR immunoreactivity was still evident in mesenchymal cells in the nephrogenic cortex (Figure 1H).

We also localized LIF and LIFR protein in adult kidneys. Cytoplasmic immunostaining for LIF was observed mainly in the collecting ducts (Figure 2, A to C), and, as shown in Figure 2B, no LIF immunoreactivity was detected in the S3 segment of the proximal tubules in the outer medulla. In mature kidneys, LIFR immunoreactivity was also predominantly detected in the collecting ducts, coinciding with the distribution of LIF protein (Figure 2, E to G). No immunostaining was observed in sections incubated with normal horse serum (Figure 2, D and H).

Expression of LIF and LIFR in the Rat Kidney after Ischemia/Reperfusion Injury

To investigate whether LIF is involved in renal tubular regeneration, we first used the real-time PCR method to quantify changes in the expression of LIF and LIFR mRNA after ischemia/reperfusion (I/R) injury.

In post-ischemic kidneys, LIF mRNA expression had increased 14.3-fold on day 1 after reperfusion, compared with its expression in pre-ischemic kidneys (Figure 3A). The increase in LIF mRNA persisted until day 7, after which gradually returned to the basal level by day 14. Interestingly, the increase in LIFR mRNA occurred later than the increase in LIF mRNA (Figure 3B). The LIFR mRNA level began to increase on day 4 and persisted until day 14, before returning to baseline by day 30.

The LIF mRNA expression in the kidneys was localized by means of *in situ* hybridization. In normal kidneys, LIF mRNA appeared to be mainly present in the collecting ducts (data not shown). At 1 d after the renal I/R injury, the hybridization signal for LIF mRNA was progressively increased, consistent with the results of the real-time PCR analysis (Figure 4, A and B). The most prominent increase in signal for LIF mRNA was noted in the tubular epithelial cells in the outer medulla, which is the site most vulnerable to ischemic injury. No positive signal was obtained with the sense cRNA probe (Figure 4C).

The LIF and LIFR proteins in the I/R-injured kidneys were precisely localized by an immunohistochemical technique. Whereas LIF protein was expressed in the collecting ducts in normal kidneys, increasingly prominent expression of LIF protein was found in the outer medulla beginning 24 h after the ischemic injury (Figure 5A). Immunostaining was particularly evident in the S3 segment of the proximal tubules, where no LIF immunoreactivity was detected under normal conditions. At higher magnification, immunoreactivity was seen in both the detached and the attached cells in the injured tubules (Figure 5B). Double-staining was performed to detect LIF expression in combination with aquaporin-1 (AQP-1), which is known to be expressed in proximal tubules, especially in the S3 segment (17,18). The results of double-staining showed that most tubules staining for LIF expressed AQP-1, however, some AQP-1–negative tubules contained LIF-positive cells (Figure 5C). This suggests that the LIF protein was predominantly localized in the S3 segments of the proximal tubules of ischemic kidneys and to some extent in the distal tubules in their outer medulla.

We then examined the relationship between LIF expression and tubular cell proliferation after I/R injury. Cell proliferation was assessed by incorporation of BrdU injected into the rats 2 h before sacrifice. BrdU-positive cells were rarely observed in normal kidney. In ischemic kidney, BrdU-positive cells were observed predominantly in the outer medulla, where damage to the tubule cells was most obvious. Double immunohistochemical staining revealed that most BrdU-positive cells were present in tubules expressing LIF (Figure 5D).

LIFR was also predominantly localized in the proximal

Figure 1. Expression of leukemia inhibitory factor (LIF) (A, C, D, E and G) and LIF receptor (LIFR) (B, F, and H) during rat kidney development. (A and B) an E15 metanephros; (C to F) E17 fetal kidneys; (G and H) newborn kidneys (P1). (A) Faint LIF immunoreactivity was detected in the ureteric buds. (B) LIFR immunoreactivity was observed predominantly in mesenchymal cells on E15. (C) On E17, LIF was expressed in the derivatives of the ureteric buds, including the tip of ureteric buds (D), and the collecting ducts in medulla (E). (F) LIFR was expressed in mesenchymal cells and ureteric buds on E17. (G) LIF immunoreactivity was localized to the collecting ducts in newborn kidney. (H) LIFR was expressed in collecting ducts and nephrogenic mesenchyme in newborn kidney. Magnifications: ×200 in A, B, C, F, G, and H; ×400 in D and E.

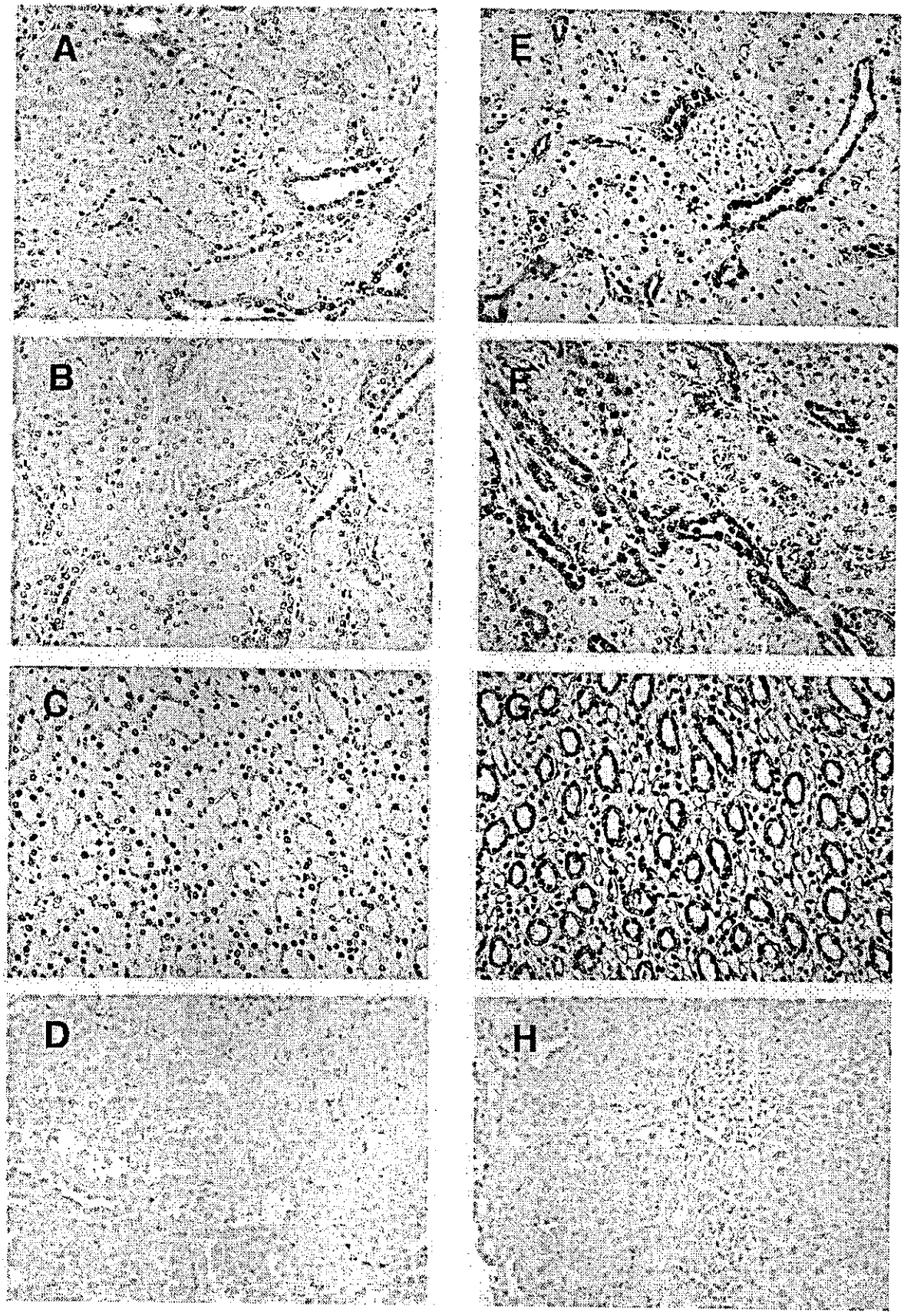
A
B
C
D
E
F
G
H

tubular cells of the outer medulla in the I/R-injured kidneys, coinciding with the distribution of LIF protein (Figure 5E).

Expression of LIF mRNA in an In Vitro *Model of Ischemic Renal Injury*

An *in vitro* model of ischemic renal injury in cultured rat renal epithelial cell line NRK 52E (19) was used to further elucidate whether LIF is involved in renal tubular regeneration. The *in vitro* model of ischemic renal injury was created by inducing ATP depletion by producing chemical anoxia with the mitochondrial inhibitor antimycin A. When monolayers of NRK 52E cells were exposed to 1 μM antimycin A, cellular levels of ATP rapidly declined to 2.1% of the control values within 30 min (Figure 6). This effect could be reversed by removing the antimycin A and restoring the regular medium. The ATP level recovered to 64.0% of the control values 3 h after ATP repletion.

The change in LIF mRNA expression during the recovery period was quantified by using the real-time PCR method (Figure 7). The LIF mRNA level began to increase on 6 h and persisted until 12 h after ATP depletion and then gradually decreased to baseline (Figure 7).

Role of LIF in Tubular Regeneration after ATP Depletion

To investigate the mitogenic effect of LIF on renal tubular cells, we assessed the effect of anti-LIF neutralizing antibody on recovery from the antimycin A-induced injury. NRK 52E cells were injured by exposure to antimycin A for 1 h and then incubated in a recovery medium containing anti-LIF neutralizing antibody. The number of surviving cells was determined 48 h after ATP depletion (Figure 8A). Blocking endogenous LIF protein with 1.0 μg/ml of anti-LIF antibody induced a significant reduction in cell number at 48 h during the recovery phase. DNA synthesis was also measured as incorporation of BrdU. In agreement with the results for cell number, 1.0 μg/ml of anti-LIF antibody lowered DNA synthesis at 24 h during recovery (Figure 8B). No significant change was observed in NRK 52E cells incubated with normal goat IgG (data not shown). To determine whether the mitogenic effect of endogenous LIF was specific to the post-injury period, we performed similar studies with uninjured NRK 52E cells. In contrast to the results in the post-injury period, anti-LIF antibody had no effect on cell number or DNA synthesis in uninjured NRK 52E cells (Figure 9).

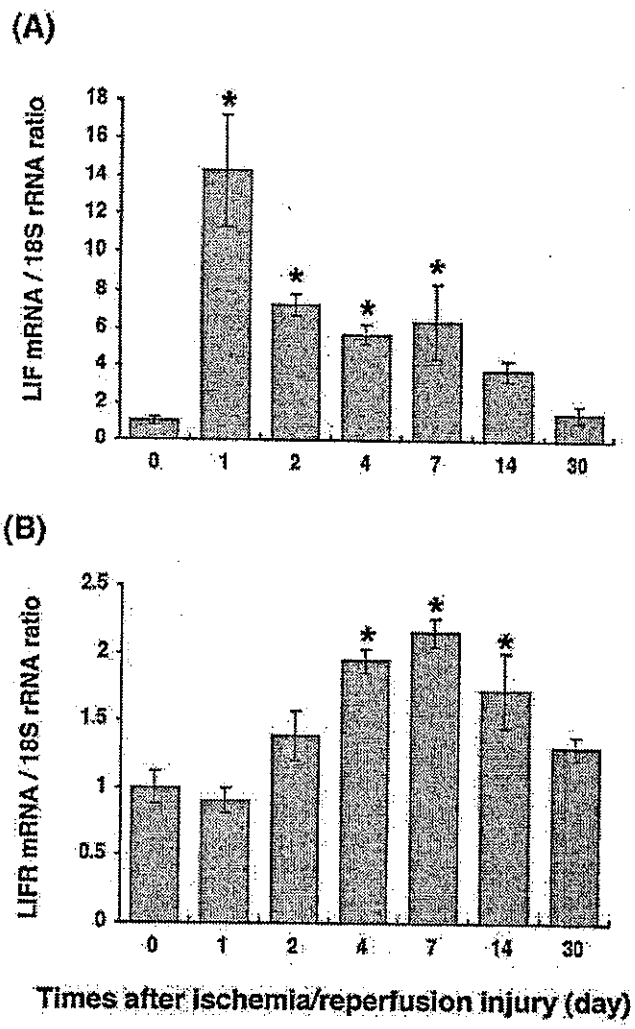

Figure 3. Expression of mRNA for LIF (A) and LIFR (B) in rat kidneys after ischemia/reperfusion (I/R) injury. Total RNA was extracted from kidneys at the indicated times after reperfusion. Quantification of mRNA was determined by real-time PCR. Expression was normalized to an endogenous control 18S ribosomal RNA (rRNA) and is shown as ratio to value of day 0. (A) LIF mRNA expression after I/R injury. (B) LIFR mRNA expression after I/R injury. Values represent means ± SEM for five or six animals. * $P < 0.05$ *versus* day 0.

Discussion

It has been suggested that regeneration processes may recapitulate developmental paradigms to restore organ or tissue function (3,4). Several genes including Pax-2, Wnt-4, and activin-A, which play a pivotal role in nephrogenesis, have been shown to be re-expressed in the kidney in the regeneration process following injury (8–11). We focused our attention on LIF, since it has been shown to play an important role in renal development (16,22). This study demonstrates for the first time that LIF participates in kidney regeneration after ischemic injury.

Figure 2. Immunohistochemical localization of LIF (A to C) and LIFR (E to G) in normal adult rat kidneys. Paraffin sections from the cortex (A, D, E and H), outer medulla (B and F), and papilla (C and G) of normal adult kidneys are presented. Immunostaining of both proteins were mainly detected in the collecting ducts in the adult rat kidney. When using normal horse serum instead of the anti-LIF antibody (D) or normal horse serum instead of the anti-LIFR antibody (H), no positive signal was observed. Magnification: ×200.

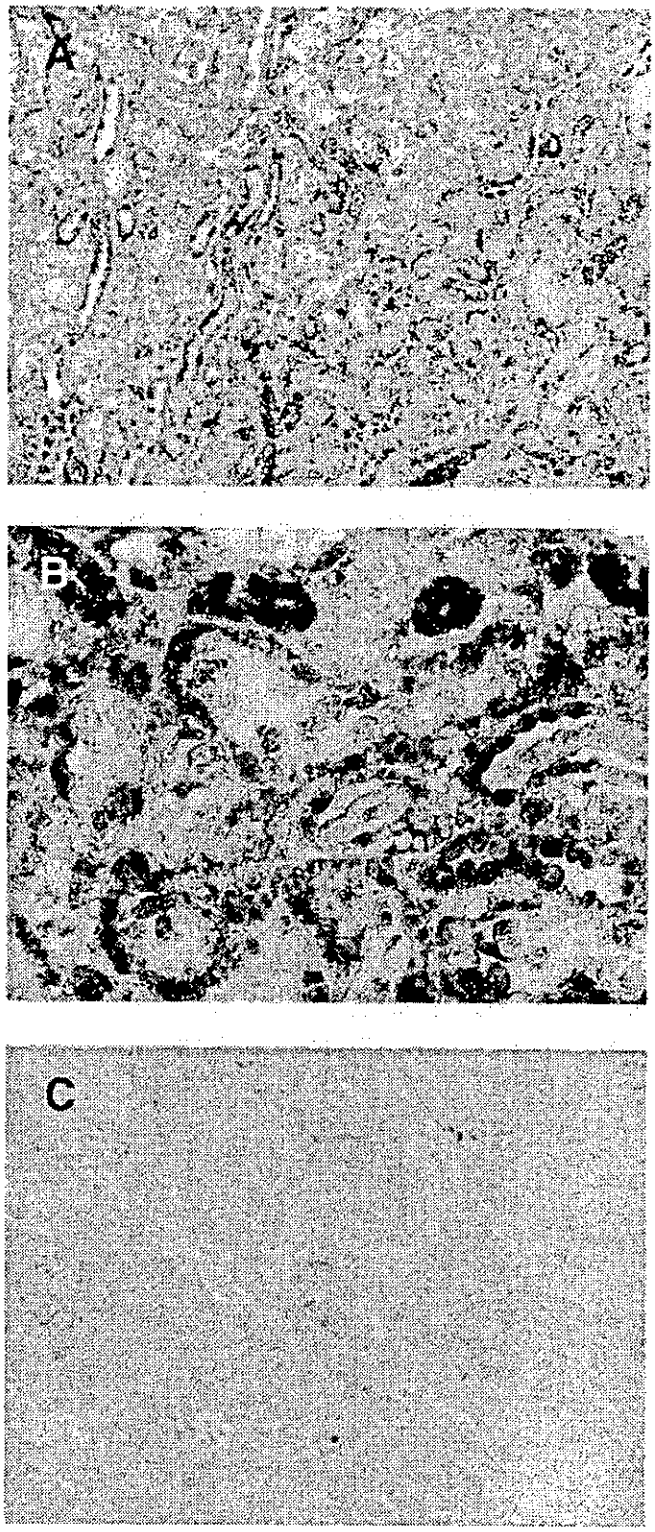

Figure 4. In situ hybridization analysis for LIF mRNA in ischemic kidney. Digoxigenin-labeled antisense (A and B) or sense (C) riboprobe was used. (A and B) Strong signal for LIF mRNA was observed in tubular cells in the outer medulla of kidney 24 h after reperfusion. (C) The sense probe for LIF yielded no positive signal. Magnifications: ×100 in A; ×400 in B and C.

The metanephros, which becomes the permanent kidney, arises from two mesodermal derivatives: the ureteric bud and the metanephric mesenchyme. Once the ureteric bud grows out from the Wolffian duct and encounters the mesenchyme, a series of reciprocal inductive events takes place that results in the ureteric bud growing and branching to form the collecting ducts, and the metanephric mesenchyme condensing and forming the tubules and the glomeruli (23). LIF secreted by the ureteric buds plays an important role in the conversion of the mesenchyme into epithelium (16,22); however, the spatiotemporal expression patterns of LIF and its receptor have not been fully elucidated. Accordingly, we first investigated the localization of LIF and LIFR in fetal and adult rat kidney.

In developing rat kidney, expression of LIF and LIFR was observed in the derivatives of the ureteric buds on E17 and thereafter. As nephrogenesis progressed, the ureteric buds differentiated into collecting ducts, which consistently expressed LIF and LIFR even after nephrogenesis had been completed. Only LIFR was expressed in the mesenchyme, with no expression of LIF in mesenchymal cells being detected in either fetal or adult kidney. LIFR expression in the mesenchymal cells was already apparent on E15, and it was sustained until the neonatal kidney.

The nephrogenic zone of the embryonic kidney is where primitive tubules and glomeruli are generated. In the nephrogenic zone, the tips of ureteric buds were observed to express LIF and LIFR, whereas the surrounding mesenchymal cells expressed LIFR. Presumably, secreted LIF binds to the LIFR located in the ureteric buds in an autocrine fashion and to the LIFR located in mesenchyme in a paracrine fashion. The LIF-LIFR system is speculated to play a pivotal role in nephrogenesis, and that would be consistent with the results reported by other investigators (16,22). In the adult kidney, expression of LIF and LIFR was most often localized in the collecting ducts. These changes in distribution suggest a different role of LIF/LIFR in the embryonic and adult kidney.

LIF is a pleiotropic cytokine that is particularly involved in growth and development. In the kidney, it is known to play an important role in nephrogenesis. In the adult, LIF has been shown to be involved in a variety of acute and chronic inflammations. LIF has been identified within the urine of renal allograft recipients during episodes of acute rejection (24). The LIF expression level in cultured mesangial cells has been shown to be increased by cytokines (25). Glomerulonephritis induces LIF in the glomeruli, and administration of exogenous LIF ameliorates glomerulonephritis (26). The function of LIF in the kidney under physiologic conditions is largely unknown, although there is a solitary report by Tomida M *et al.* (27) on the action of LIF on renal tubule cells. They found that LIF inhibits the development of Na^+–dependent hexose transport in LLC-PK1 cell, which was isolated from pig kidney and is thought to have the characteristics of proximal tubule cells. In our study, LIF was found to be predominantly expressed in the collecting duct cells. The findings of Tomida *et al.* (27) and our own suggest that LIF may be involved in ion transport in renal collecting ducts.

Next, we tested the hypothesis that LIF is involved in the

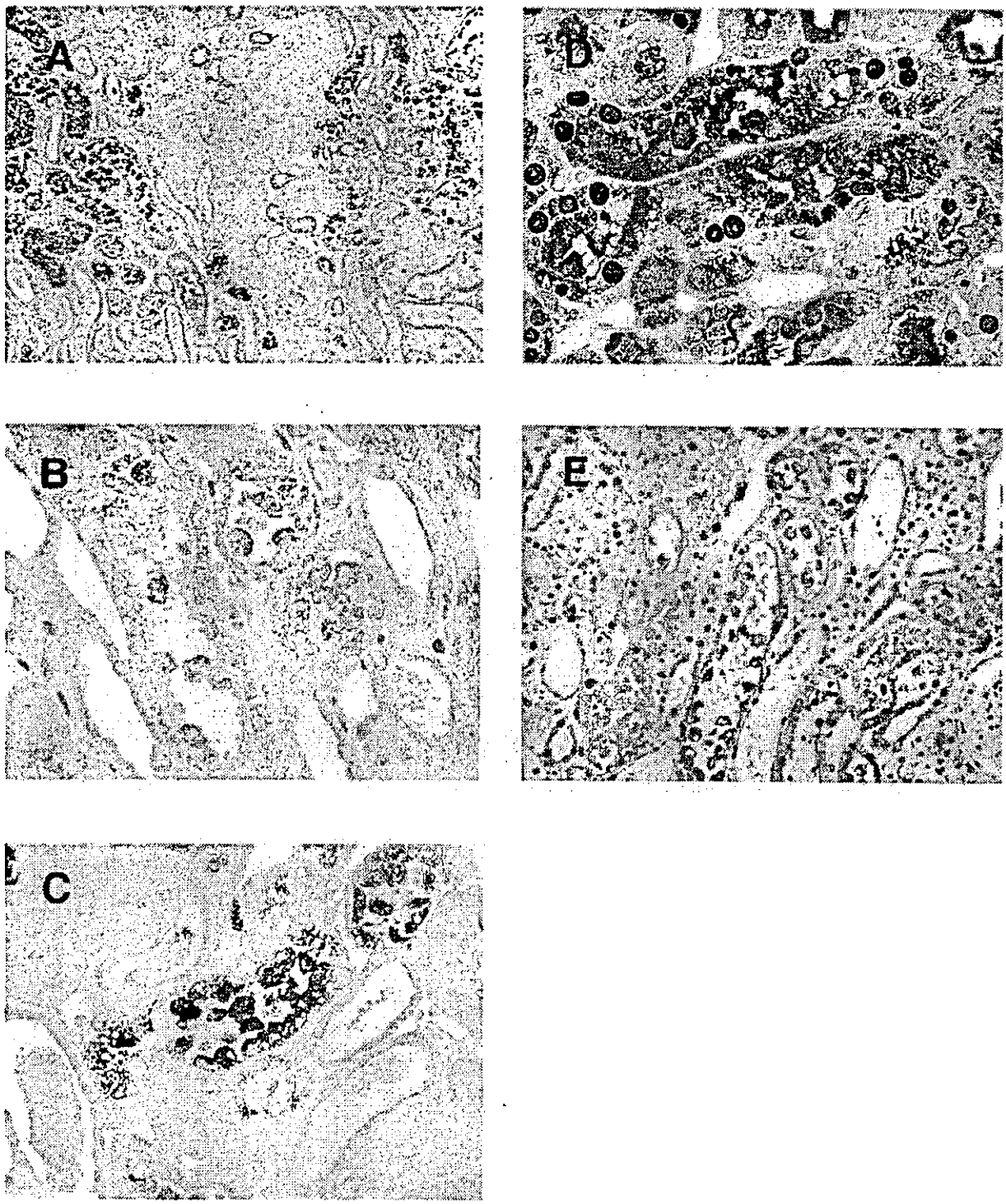

Figure 5. Immunohistochemical localization for LIF and LIF receptor protein in ischemia/reperfusion-injured kidneys 24 h after reperfusion. (A and B) Immunohistochemical localization for LIF protein (brown staining) in the outer medulla of ischemic kidneys. The dramatic increase in LIF immunostaining in injured epithelial tubular cells, especially of S3 segment of the proximal tubules. Detached cells and attached cells in the tubules were stained. (C) Double immunohistochemistry for LIF and aquaporin-1 (AQP-1), marker of proximal tubules. Note that LIF (purple staining) was co-localized with AQP-1 (blue staining). (D) Double immunohistochemistry for LIF and BrdU. BrdU were injected with rat 2 h before sacrifice. Most BrdU staining (brown nuclear staining) was found in proximal tubules expressing LIF (purple cytoplasmic staining). (E) Immunohistochemical localization for LIF receptor (brown staining) in the outer medulla of ischemic kidneys. The expression pattern is similar to that of LIF. Magnifications: ×100 in A; ×400 in B–D; ×200 in E.

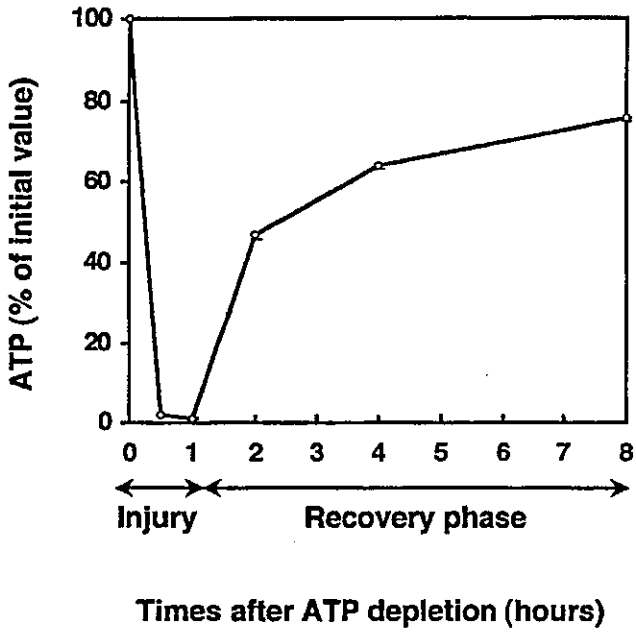

Figure 6. Cellular ATP levels after chemical anoxia using antimycin A in NRK 52E cells. Confluent NRK 52E cells were incubated in Dulbecco PBS with 1.5 mM $CaCl_2$, 2 mM $MgCl_2$, and either 1 μM antimycin A. Intracellular ATP levels were measured by a luciferase-based assay at the indicated time after ATP depletion. Values are expressed as a percentage of the value of pre-injury and represent means ± SEM from three separate experiments.

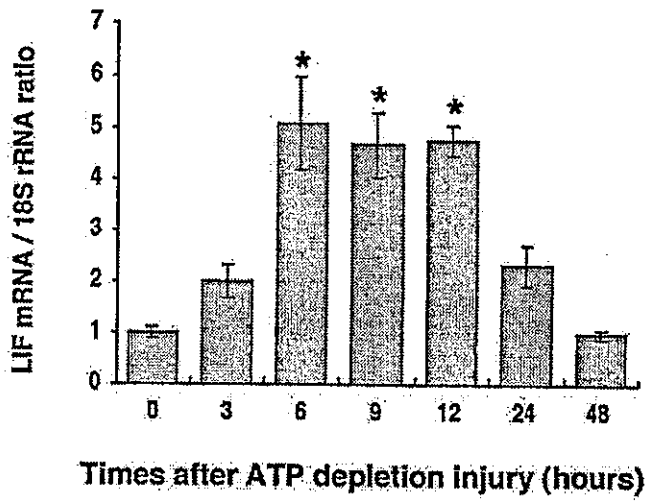

Figure 7. Expression levels of mRNA for LIF in NRK 52E cells after ATP depletion. Total RNA was extracted from cells at the indicated times after ATP depletion. Quantification of mRNA was determined by real-time PCR. Expression levels were normalized to an endogenous control 18S ribosomal RNA (rRNA) and are shown as ratio to the value of 0 h. Values represent means ± SEM for four independent experiments.

process of kidney regeneration after injury by investigating expression of LIF and LIFR during the recovery phase from injury by real-time PCR, *in situ* hybridization, and immunohistochemistry in a model of acute renal failure created by inducing ischemia. Our first finding in the ischemic kidneys was that the increase in LIF mRNA expression began on day 1 after the injury and was sustained for 7 d, whereas the increase in LIFR mRNA expression was observed several days later. Many genes have been reported to be upregulated after tubular injury. *Egr-1* (28), *c-fos* (28), *c-myc* (29), and the genes encoding heat shock protein-70 (30) and parathyroid hormone–related protein (PTHrP) (31) have been shown to be upregulated in the very early phase after injury. Their upregulation was detected as early as within a few hours and returned to baseline within 1 d. These are considered the early response genes to renal injury. The increase in gene expression of Pax-2 (8,11), activin-A (10), platelet-derived growth factor (PDGF) (32), ciliary neurotrophic factor (CNTF) (33), hepatocyte growth factor receptor (c-Met) (34), galectin-3 (35), and transforming growth factor–β1 (TGF-β1) (36) persisted for several days, and these genes are thought to be responsible for tubular regeneration. The upregulation of LIF was observed on 1 d after the ischemic insult and persisted for 7 d. Its time course suggests that LIF participates in the regeneration process. Interestingly, there was a time lag between the gene upregulation of LIF and LIFR, and there is a possibility that LIF itself or some other molecules in the downstream of LIF signaling may stimulate the transcription of LIFR.

We did not perfuse the kidney to remove the blood before total RNA isolation. The possibility of contamination by RNA from blood cells cannot be ruled out, however, any contribution by blood cells to the increase in LIF mRNA is thought to be minimal. The increase in LIF expression is mainly attributable to the regenerating epithelial tubular cells, and this is supported by two observations. First, immunohistochemistry and *in situ* hybridization studies showed the most prominent staining of LIF in the epithelial cells. Second, *in vitro* study in the absence of blood cells demonstrated upregulation of LIF mRNA.

Our second observation in the ischemic kidneys was that the increase in expression of LIF and LIFR was predominantly in the outer medulla, especially in the S3 segment of the proximal tubules, where LIF or LIFR is not usually expressed. The outer medulla is also the most prominent site of ischemia-induced acute tubular necrosis and subsequent DNA synthesis (29,37). In our study, most of the cells that stained with BrdU were found in LIF/LIFR-positive tubules. Interestingly, LIF and LIFR were expressed in the detached cells as well as the attached cells of S3 segment of the proximal tubules, and in previous studies, c-Met (34), galectin-3 (35), TGF-β1 (36), and PDGF (32) were shown to be expressed strongly in the detached cells of S3 proximal tubules. By the same analogy as in the speculations about these genes, the increase in LIF staining in the detached cells presumably reflects an unsuccessful protective response to injury before the cells' detachment and necrosis.

Although LIF expression is restricted to the ureteric bud and

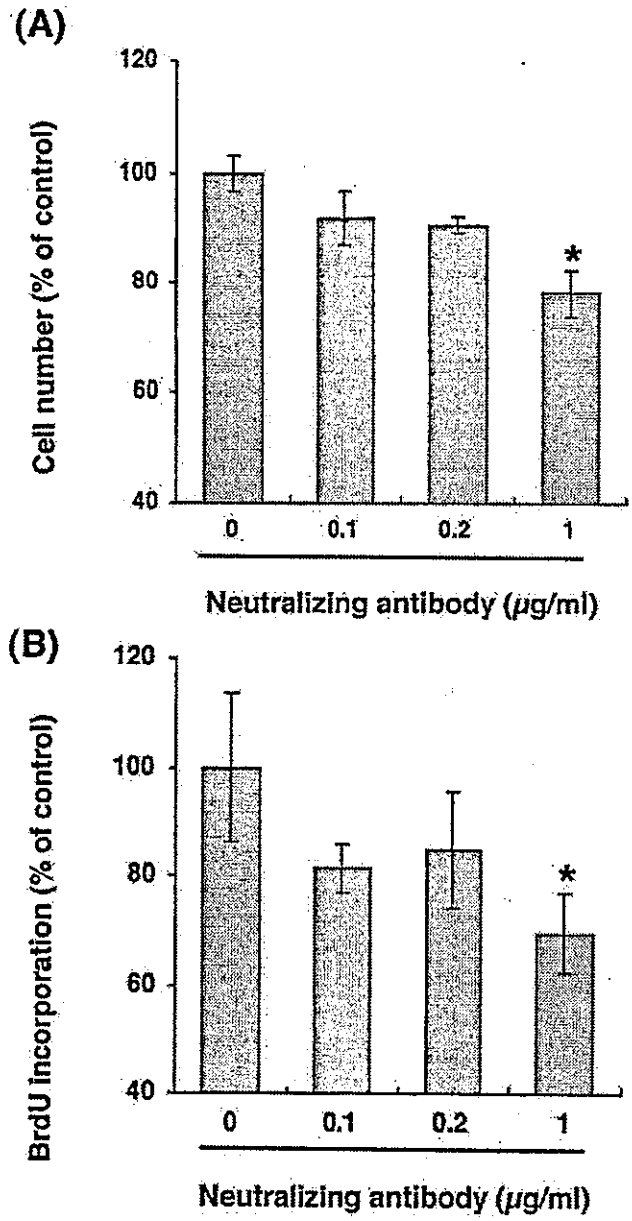

Figure 8. The effect of anti-LIF neutralizing antibody on recovery from ATP depletion in NRK 52E cells. The injured cells were allowed to recover in regular growth medium containing 0, 0.1, 0.2, or 1.0 μg/ml of anti-LIF antibody. (A) Cell number on day 2 ($n = 4$) and (B) BrdU incorporation on day 1 ($n = 6$) after ATP depletion were decreased by 1.0 μg/ml of anti-LIF antibody. The values are indicated as percentage of the value without anti-LIF antibody, and means ± SEM. * $P < 0.05$ *versus* the value without anti-LIF antibody.

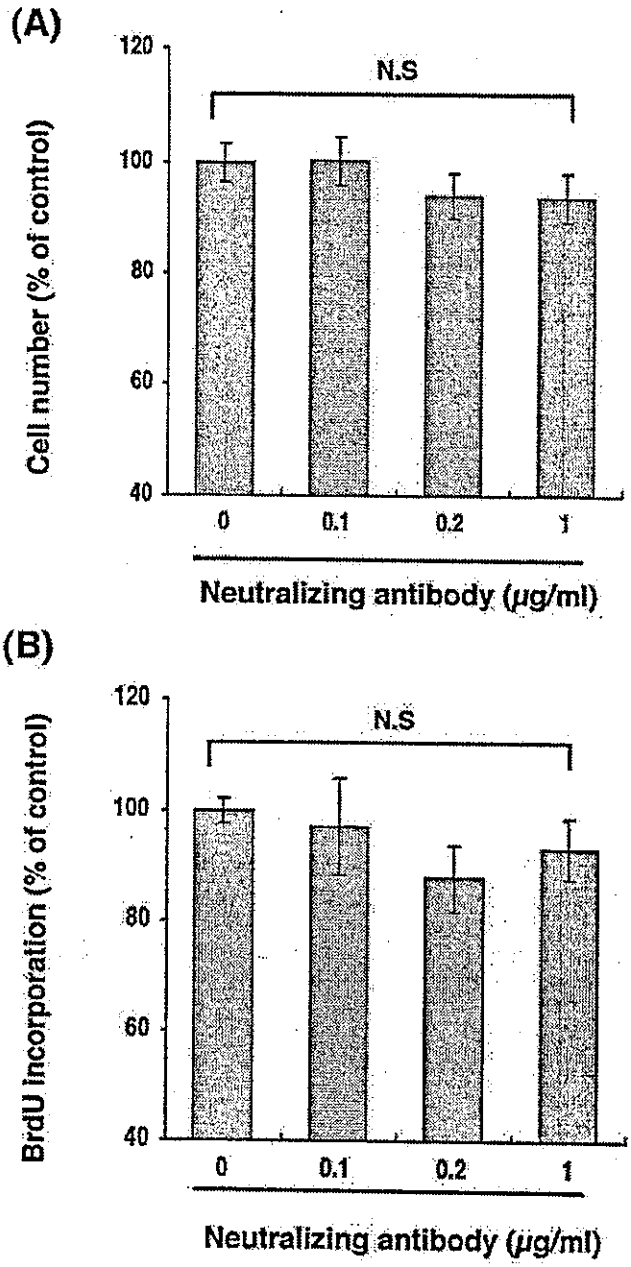

Figure 9. The effect of anti-LIF neutralizing antibody on proliferation in NRK 52E cells. The non-injured cells were incubated in regular growth medium containing 0, 0.1, 0.2, or 1.0 μg/ml of anti-LIF antibody. (A) Cell number on day 2 ($n = 4$) or (B) BrdU incorporation on day 1 ($n = 6$) were not changed. The values are indicated as percentage of the value without anti-LIF antibody and means ± SEM. NS, no significant difference.

its derivatives, the major site of action of LIF is the mesenchyme. LIF is excreted by the ureteric bud and induces a mesenchymal to epithelial conversion via binding to its receptor located in the mesenchyme. Thus, LIF is important to the development of metanephric mesenchyme-derived structures. In view of this, the involvement of LIF in regeneration of the injured proximal tubules, which are derived from the mesenchyme, is consistent with the functional role of LIF in developing kidney. However, we do not know why LIF is expressed in bud-derived structures during development and re-expressed in mesenchyme-derived structures in disease. The expression pattern of galectin-3 is similar to that of LIF. Galectin-3 is